AKT-MEDIATED REGULATION OF ANTIDEPRESSANT-SENSITIVE SEROTONIN TRANSPORTER FUNCTION, CELL SURFACE EXPRESSION AND PHOSPHORYLATION

Jeyaganesh Rajamanickam[*1], Balasubramaniam Annamalai[†1], Troels Rahbek-Clemmensen[‡1], Santhanalakshmi Sundaramurthy[*1], Ulrik Gether[‡], Lankupalle D. Jayanthi[*] and Sammanda Ramamoorthy[*2]

[*]Department of Pharmacology and Toxicology, Virginia Commonwealth University, Richmond, VA 23298, USA

[†]Department of Neurosciences, Medical University of South Carolina, Charleston, SC 29425, USA

[‡]Molecular Neuropharmacology and Genetics Laboratory and the Lundbeck Foundation Center for Biomembranes in Nanomedicine, Department of Neuroscience and Pharmacology, Faculty of Health and Medical Sciences, Panum Institute, University of Copenhagen, DK-2200 Copenhagen, Denmark

[1]These authors have contributed equally to this study.

[2]To whom correspondence should be addressed: Sammanda Ramamoorthy, Department of Pharmacology and Toxicology, Virginia Commonwealth University, Richmond, VA 23298. Tel.: 804-828-8407; Fax: 804-828-2117; Email: sramamoorthy@vcu.edu

Running Title: Akt regulation of serotonin transporter

Keywords: Monoamine transporters, Uptake, Antidepressants, Protein Kinase B, Trafficking, Phosphorylation

Abbreviations:

5-HT, 5-hydorxytryptamine (serotonin); Akt, protein kinase B/Akt; Akt X, Akt inhibitor X (10-(4′-(N-diethylamino)butyl)-2-chlorophenoxazine); Akt1 inhibitor A-674563, (2S)-1-(5-(3-methyl-1H-indazol-5-yl)pyridin-3-yloxy)-3-phenylpropan-2-amine; Akt2 inhibitor CCT128930, 4-(4-chlorobenzyl)-1-(7H-pyrrolo[2,3-d]pyrimidin-4-yl)piperidin-4-amine; BIO, (6-bromoindirubin-3'-oxime); CHIR99021 (6-[[2-[[4-(2,4-Dichlorophenyl)-5-(5-methyl-1H-imidazol-2-yl)-2-pyrimidinyl]amino]ethyl]amino]-3-pyridinecarbonitrile); DMEM, Dulbecco's modified Eagle's medium; EGFP, enhanced green fluorescent protein; ERGIC, Endoplasmic reticulum Golgi-intermediate compartment; GSK3α/β, glycogen synthase kinase-3α/ß; GPCRs, G-protein coupled receptors; HEK 293 Cells, human embryonic kidney cells; hSERT, human SERT; KRH, Krebs-Ringer-HEPES buffer; MDMA, 3,4 –methylenedioxymethampetamine; hp38 MAPK, p38 mitogen-activated protein kinase; PAGE, polyacrylamide gel electrophoresis; PBS, phosphate buffered saline; PI3K, phosphatidylinositol-3-kinase; PKA, protein kinase A; PKC, protein kinase C; PKG, protein kinase G; RIPA, radioimmunoprecipitation assay lysis buffer; SSRI, serotonin selective reuptake inhibitors; SERT, serotonin transporter; TDZD-8,(4-Benzyl-2-methyl-1,2,4-thiadiazolidine-3,5-dione).

Biochemical Journal Immediate Publication. Published on 11 Mar 2015 as manuscript BJ20140826

ABSTRACT

The serotonin (5-HT) transporter (SERT) controls serotonergic neurotransmission in the brain by rapid clearance of 5-HT from the synaptic cleft into presynaptic neurons. SERTs are primary target for antidepressants for therapeutic intervention of mood disorders. Our previous studies have identified the involvement of several signaling pathways and protein kinases in regulating SERT function, trafficking and phosphorylation. However, whether the protein kinase B/Akt regulates SERT function is not known. Here, we made novel observation that inhibition of Akt resulted in the down regulation of SERT function through the regulation of SERT trafficking and phosphorylation. Akt inhibitor Akt X reduced the endogenously phosphorylated Akt and significantly decreased 5-HT uptake and 5-HT uptake capacity. Furthermore, SERT activity is also reduced by small interfering RNA downregulation of total and phospho-Akt levels. The reduction in SERT activity is paralleled by lower level of surface SERT protein, reduced SERT exocytosis with no effect on SERT endocytosis and accumulation of SERT in intracellular endocytic compartments with the most prominent localization to late endosomes and lysosomes. Akt2 inhibitor was more effective than Akt1 inhibitor in inhibiting SERT activity. Inhibition of downstream Akt kinase GSK3α/ß stimulates SERT function. Akt inhibition leads to decrease in SERT basal phosphorylation. Our results provide evidence that Akt regulates SERT function and cell surface expression by regulating the intracellular SERT distribution and plasma membrane availability, which perhaps may be linked to SERT phosphorylation state. Thus, any changes in the activation of Akt and/or GSK3α/ß could alter SERT mediated 5-HT clearance and subsequently serotonergic neurotransmission.

Summary Statement

The present study is focused on the cellular basis for Akt mediated SERT regulation. SERT has been implicated in mood disorders. SERT is a primary target for antidepressants used in the therapeutic intervention of psychiatric disorders.

Biochemical Journal Immediate Publication. Published on 11 Mar 2015 as manuscript BJ20140826

INTRODUCTION

The serotonin (5-HT) transporter (SERT) expressed in presynaptic serotonergic neurons controls 5-HT neurotransmission by rapid reuptake of released 5-HT [1-3]. 5-HT transport is of clinical relevance because SERT is a high affinity target for antidepressants such as serotonin selective reuptake inhibitors (SSRIs) [3, 4]. SSRIs are used successfully to treat several psychiatric disorders. Furthermore, SERT is one of the high affinity molecular targets for drugs of abuse such as cocaine and 3,4 –methylenedioxymethampetamine (MDMA or "Ecstasy") [5]. Documentation of altered SERT expression in various types of psychopathology indicates the importance of SERT in maintaining normal brain function [6-9]. Studies from our laboratory and others revealed that the SERT-mediated 5-HT clearance is orchestrated through multiple regulatory pathways that dictate SERT-gene transcription, expression, catalytic activity, trafficking, phosphorylation, protein-protein interactions and degradation (reviewed in [10] reference therein). For example, the function of native and heterologously expressed SERT is rapidly inhibited in response to acute depletion of intracellular Ca^{2+}, inhibition of calmodulin, CaMKII, Src-kinase, p38 MAPK and activation of PKC [11-17]. On the other hand, increased intracellular Ca^{2+}, activation of NOS/cGMP, Src-kinase and MAPK pathways stimulate SERT activity [16, 18-21]. Receptor-mediated regulation of SERT has also been documented. Activation of adenosine receptors (AR), 5-HT_{1B}, atypical histamine receptors and BDNF/TrkB stimulates SERT activity [22-27] whereas stimulation of $\alpha 2$ adrenergic receptor signaling cascades reduces 5-HT uptake [28]. In addition, SERT-substrates and inhibitors can also influence kinase/phosphatase mediated SERT regulation [29].

The serine/threonine protein kinase B (PKB), also known as Akt (Akt/PKB) has been implicated in the pathogenesis of serotonin-related disorders [30-32] Activated Akt phosphorylates glycogen synthase kinase-3α/ß (GSK3α and GSK3ß) resulting in the inactivation of GSK3 [33]. SSRIs and other drugs acting on 5-HT neurotransmission have shown to inhibit GSK3ß by Akt-linked phosphorylation site [34-36]. Interestingly, altered Akt/GSK3ß pathways have been implicated in major depressive disorders [32, 37]. Given the pivotal role of SERT activity in regulating 5-HT neurotransmission, it is possible that the physiological effect of 5-HT may also be regulated through Akt-linked SERT regulation. However, presently it is not known whether the Akt regulates 5-HT uptake through regulating SERT. In the current study, we explored the role of Akt in SERT regulation and demonstrate the time and dose dependent reduction of SERT activity by Akt phospho-inhibitor Akt X. Both pharmacological and genetic reductions of Akt phosphorylation reduced SERT activity. The reduction of SERT activity is correlated with reduced cell surface expression and basal phosphorylation of SERT that could be linked to reduced plasma membrane delivery. These results suggest that constitutively active Akt controls SERT expression and function by a phosphorylation-dependent trafficking mechanism.

EXPERIMENTAL

MATERIALS

Akt inhibitor Akt X was purchased from EMD Millipore (Billerica, MA). Akt1 inhibitor A-674563 and Akt2 inhibitor CCT128930 were purchased from selleckchem (Houston, TX). ECL reagents, Sulfosuccinimidyl-2-(biotinamido)ethyl-1,3-dithiopropionate (EZ link NHS-Sulfo-SS-biotin), Sulfo-NHS-Acetate and NeutrAvidin Agarose were from Pierce (Rockford, IL). 5-Hydroxy-[^{3}H] tryptamine creatinine sulfate ([^{3}H]5-HT; 28.1Ci/mmol), $^{32}PO_4$ carrier-free orthophosphate, Optiphase Supermix, and Kodak BioMax Ms-1 films were from PerkinElmer Inc. (Waltham, MA). Reagents for SDS-polyacrylamide gel electrophoresis and Bradford protein assay were obtained from Bio-Rad (Hercules, CA). Lipofectamine^{TM} 2000, DMEM and all other cell culture media were purchased from Invitrogen/Life Technologies, (Grand Island, NY). Fetal bovine serum was from Hyclone/GE Healthcare Life Sciences (Logan, UT). ON-TARGETplus SMARTpool specific to Akt1 and On-Targetplus-non targeting siRNA were purchased from Thermo Scientific Dharmacon (Lafayette, CO). SuperSignal West Pico Chemiluminescent substrate was from Thermo Fisher Scientific Inc., (Rockford, IL). Protein A Sepharose was from GE Healthcare Life Sciences (Pittsburgh, PA). GSK3α/β inhibitors BIO, CHIR-99021 and TDZD-8 were obtained from Sigma-Aldrich (St. Louis, MO). All other chemicals were obtained from Sigma-Aldrich (St. Louis, MO) or Fisher Scientific (Pittsburgh, PA) unless otherwise indicated. The following antibodies were used: Anti-calnexin was from BD Biosciences (San Jose, CA). Anti-rabbit monoclonal-Akt antibody (clone AW24) and anti-phopho-Akt (Ser473) antibody (clone 11E6) were from EMD Millipore (Billerica, MA). GSK3 antibody sampler kit was purchased from Cell Signaling (Beverly, MA). Rabbit anti-ERGIC53 was from Sigma-Aldrich (St. Louis, MO). Rabbit anti-Lamp1 was from Abcam (Cambridge UK,). Polyclonal rabbit anti-giantin was from Covance Research Products (Denver, PA). Polyclonal goat anti-SERT ST(C-20) was from Santa Cruz (Dallas, TX). HRP-conjugated secondary antibodies were from Jackson ImmunoResearch Laboratories (West Grove, PA). Fluorescently-tagged antibodies (donkey anti-Rabbit-Alexa488 and anti-goat-Alexa568) were from Invitrogen (Carlsbad, CA) Rabbit polyclonal SERT antibody (SR-12) was generated by our laboratory. In our previous studies, the use and specificity of SR-12 SERT antibody were thoroughly characterized [15, 16, 21].

METHODS

Molecular biology

The coding sequence of hSERT was inserted into the mammalian expression vector pcDNA3.1(-) (Invitrogen) using XbaI and HindIII restriction sites. The EGFP-tagged Rab5, Rab7, and Rab11 constructs (pEGFP-C1 Rab5, pEGFP-C1 Rab7, and pEGFP-C1 Rab11) were a kind gift from Dr. Kathrine W. Roche, NINDS, National Institutes of Health, Bethesda, MD [38]. The pEGFP-Rab4 plasmid was a kind gift from Dr. Jose A. Esteban, Universidad Autonoma de Madrid, Madrid, Spain [39]

Cell culture and transfections

HEK 293 (human embryonic kidney) cells were cultured in Dulbecco's modified Eagle's media (DMEM) supplemented with (v/v) 10% fetal bovine serum, 1% penicillin-streptomycin and 1% glutamine. For transient transfection experiments, cells were trypsinized and seeded in poly-D-lysine coated 24 well plates (100,000 cells/well) or 12 well plates (250,000 cells/well) and incubated at 37°C for 24 hours in

a humidified CO_2 incubator (5% CO_2). The cells were transfected with 150 ng/well (24 well plate) or 500 ng/well (24 well plate) of hSERT cDNA and/or empty pcDNA3.0 vector using lipofectamine 2000 according to manufacturer's instruction. Experiments were performed 24-28 hours after transfection [16]. For microscopy, cells were transfected 48 hours prior to experiments using 1 µg pcDNA3 hSERT + 1 µg empty vector pcDNA3 in 75 cm^2 flasks or 0.5 µg pcDNA3 hSERT + 0.25 µg empty vector pcDNA3 + 0.25 µg pEGFP-Rab4, -5a, -7, or -11 in 25 cm^2 flasks using Lipofectamine 2000. On the day before experiments, 750,000 cells/well were seeded on poly-ornithine coated coverslips in 6 well plates.

[^{3}H]5-HT uptake (SERT) assay

5-HT uptake was performed as described previously [16, 21]. The transfected cells grown in 24 well plate were washed and incubated with 1 ml of serum-free DMEM media at 37°C for 2 hours. Cells were then washed with 1 ml of prewarmed (37˚C) Krebs-Ringer-HEPES buffer (KRH, 120 mM NaCl, 4.7 mM KCl, 1.2 mM KH_2PO_4, 1.2 mM $MgSO_4$ and 10 mM HEPES, pH 7.4) on a heating block (37°C) and treated with modulators in 500µl of assay buffer (KRH solution containing 0.1 mM ascorbic acid and 0.1 mM pargyline) at 37°C for various time periods or concentrations as indicated under figure legends. The uptake assay was started by incubating the cells with 50 nM of radiolabeled [^{3}H]5-HT at 37°C for 5 min. The uptake was terminated by removing the radiolabeled substrate followed by washing the cells twice with KRH buffer. Nonspecific [^{3}H]5-HT uptake was defined as the accumulation in the presence of 10 nM fluoxetine and was subtracted from the total counts. Nonspecific background was also compared with cells transfected with pcDNA vector alone. The cells were lysed with 400 µl of Optiphase Supermix by shaking the plate for 30 min. The radioactivity was measured using MicroBeta2 LumiJET liquid scintillation counter (PerkinElmer Inc., Waltham, MA). Data are represented as the means ± S.E.M from three experiments performed in duplicate or triplicate on different batches of HEK 293 cells.

SERT kinetics

The HEK 293 cells transfected with hSERT cDNA were pretreated with Akt X (20 µM) for 30 min at 37°C. The cells were incubated with the mixture of [^{3}H]5-HT and unlabeled 5-HT from 50 nM to 5 µM for 5 min and washed with KRH solution twice. Non-specific [^{3}H]5-HT uptake was determined as the accumulation in the presence of 10 nM fluoxetine and was subtracted from total uptake. The radioactivity was measured using liquid scintillation counter. For kinetic analysis of 5-HT uptake, the values were plotted as femtomol of 5-HT uptake against the concentration of 5-HT and the data represent the means ± S.E.M from three experiments performed in triplicate on different batches of HEK 293 cells as described previously by our laboratory [16, 21]. Substrate Km and V_{max} values for 5-HT uptake were determined by nonlinear least square fits (Prism GraphPad Software Inc., La Jolla, CA) with generalized Michaelis-Menten equation: $V=V_{max}[S]^n/(K^n_m+[S]^n)$, where V = transport velocity, [S] = substrate (5-HT) concentration, and n represents the Hill coefficient.

Cell surface biotinylation to determine cell surface SERT density

Cell surface biotinylation and immunoblot analyses were utilized to determine the plasma membrane density of SERT protein as described previously [16, 21]. hSERT cDNA transfected HEK 293 cells grown in 12 well plates were pretreated with Akt X

(20 μM) for 45 min at 37°C. The cells were washed with 1 ml of ice-cold PBS/Ca-Mg buffer (138 mM NaCl, 2.7 mM KCl, 1.5 mM KH_2PO_4, 9.6 mM Na_2HPO_4, 1 mM $MgCl_2$ and 0.1 mM $CaCl_2$, pH 7.3) and incubated twice with 1 ml of EZ-link sulfo-NHS-SS-biotin (0.5 mg/ml, w/v) solution on ice for 20 min. The cells were washed with 1ml of ice-cold PBS-Ca^{2+}-Mg^{2+} buffer and the biotinylation was quenched by incubating the cells with 100 mM of glycine in PBS/Ca-Mg buffer for 15 min at 4°C. The cells were washed again with ice-cold PBS/Ca-Mg buffer. The cells were lysed with 400 μl of cold RIPA lysis buffer (10 mM Tris-HCl, pH 7.5, 300 mM NaCl, 1 mM EDTA, 1% Triton X-100 (v/v), 1% SDS (w/v), and 0.1% sodium deoxycholate (w/v)) supplemented with protease inhibitors (1 μg/ml aprotinin, 1 μg/ml leupeptin, 1 μM pepstatin, and 250 μM phenylmethylsulfonyl fluoride) and phosphatase inhibitors (10 mM sodium fluoride, 50 mM sodium pyrophosphate and 5 mM activated orthovanadate) by shaking plate at 4°C for one hour and by passing through a 26-gauge needle 6 times. The lysed cells were centrifuged at 25,000 g for 30 min. The supernatant was collected in fresh microtubes and concentration of the protein was measured using Bradford assay. NeutrAvidin beads were washed twice with ice-cold PBS/Ca-Mg buffer and once with ice-cold RIPA buffer. Equal amounts of biotinylated samples were incubated with 60 μl of NeutrAvidin beads at 4°C on a nutator for overnight. Next day, the samples were washed with RIPA buffer three times. The biotinylated proteins were eluted in 45 μl of 2X Laemmli buffer (62.5 mM Tris-HCl, pH 6.8, 20% glycerol (v/v), 2% SDS (w/v), 0.01% bromophenol blue (w/v) and 5% β-mercaptoethanol (v/v)) and separated by 10% SDS-PAGE along with total extracts and unbound fractions, transferred to polyvinylidene difluoride membrane and probed with SERT specific SR-12 antibody as described previously by us [21]. The immunoreactive proteins were visualized using ECL or ECL plus reagent. Subsequently, the blots were stripped and reprobed with anti-calnexin antibody to validate the surface biotinylation of plasma membrane proteins as well as loading protein levels. SERT densities from total, nonbiotinylated (representing the intracellular pool) and biotinylated (representing the surface pool) fractions were normalized using total levels of SERT as well as levels of calnexin in the total extract. Multiple exposures were evaluated by digital quantitation using NIH ImageJ (version 1.48v) software to ensure that results were within the linear range of the film exposure.

Assay of SERT delivery into the plasma membrane

Plasma membrane insertion of SERT (exocytosis) assay was performed using biotinylation and immunoblotting as described previously [40, 41]. Briefly, HEK 293 cells transfected with hSERT cDNA were grown in 12 well plates, cooled rapidly to 4°C by washing with ice-cold PBS/Ca-Mg buffer and incubated with Sulfo-NHS-Acetate (1mg/ml) in ice-cold PBS/Ca-Mg buffer for 1 hour at 4°C (trafficking nonpermissive condition) to block all free amino groups [42, 43]. After washing away the sulfo-NHS-acetate with cold PBS/Ca-Mg buffer, the cell membrane impermeable sulfo-NHS-SS-biotin (1 mg/ml) in PBS/Ca-Mg containing the vehicle or Akt X (pre-warmed at 37˚C) was added to the cells and incubated further for indicated time periods at 37˚C (trafficking permissive condition). At end of the each time period, the cells were rapidly cooled to 4°C and incubated twice with 100 mM glycine in ice-cold PBS/Ca-Mg buffer for 15 min. One dish of cell was incubated at 4°C as an experimental control. Biotinylated SERTs inserted into the plasma membrane (surface) and nonbiotinylated (intracellular) SERT were analyzed by immunoblotting

with SR-12 SERT antibody and quantified as described under *"Cell surface biotinylation to determine cell surface SERT density".*

Reversible biotinylation to determine SERT internalization

A reversible biotinylation technique was performed to determine the effect of Akt X on internalization (endocytosis) of SERT as described previously by us [40, 41]. hSERT cDNA transfected HEK 293 cells grown in 30 mm dish were cooled rapidly to 4°C to inhibit endocytosis by washing with ice-cold PBS/Ca-Mg buffer and surface biotinylated with a disulfide-cleavable biotin (sulfo-NHS-SS-biotin) and free biotinylating reagent was removed by quenching with glycine. SERT endocytosis was initiated by incubating the cells with prewarmed PBS/Ca-Mg buffer with vehicle or Akt X (20 μM) at 37°C for indicated time periods. At the end of each time point, the cells were rapidly cooled to 4°C and washed with ice-cold PBS/Ca-Mg buffer to stop the endocytosis. The cells were then washed and incubated twice with 50 μM sodium 2-mercapto-ethanesulfonate (MesNa), a reducing agent in PBS/Ca-Mg buffer for 20 min to dissociate the biotin from cell surface-resident proteins via disulfide exchange. To define total biotinylated SERTs, one dish of biotinylated cells was not subjected to reduction with MesNa, and directly processed for extraction followed by isolation by NeutrAvidin beads. To define MesNa-accessible SERTs, another dish of cells was treated with MesNa immediately (at 0 time) following biotinylation at 4°C to reveal the quantity of surface SERT biotinylation that MesNa can reverse efficiently. The cells were lysed and biotinylated proteins were separated by using NeutrAvidin beads and subjected to immunoblotting as described under *"Cell surface biotinylation to determine cell surface SERT density".*

siRNA interference of Akt

The Akt interference was performed in HEK 293 cells with ON-*TARGETplus SMARTpool siRNAs* specific to Akt. The nonspecific scrambled siRNA was used as a control. siRNA duplexes (30 nM) were transfected into cells using lipofectamine 2000 according to manufacturer's instructions. After 16 hours post siRNA transfection, HEK 293 cells were then transfected with hSERT cDNA. After 24 hours, 5-HT uptake assay was performed as described under *"[^{3}H]5-HT uptake (SERT) assay"*. In parallel, immunoblot analysis of total and phospho-Akt was carried out to verify the suppression of Akt levels. The same blot was reprobed for calnexin antibody to determine the nonspecific effect of siRNAs as described previously [16, 21].

Phospho and total Akt and GSK3α/ß levels

After pretreatment of HEK 293 cells expressing hSERT with modulators as indicated under figure legends or the HEK 293 cells that were transfected with siRNA specific to Akt or scrambled siRNA were lysed with RIPA buffer containing phosphatase inhibitors (10 mM NaF, 10 mM sodium pyrophosphate, 1 mM sodium orthovanadate, 1 μM okadaic acid) and 0.1% protease inhibitor cocktail (v/v) to quantify total and phopho-Akt and GSK3α/ß levels. Lysates were centrifuged at 25,000 g for 30 min at 4°C and supernatant was collected for immunoblotting analysis. Proteins were incubated with Laemmli sample buffer and separated by 10% SDS-PAGE. The separated proteins were transferred to polyvinylidene difluoride membrane and probed with anti-phospho Akt or anti-phospho GSK3α/ß antibodies to detect

phospho-Akt and GSK3α/ß levels. The same blots were then stripped and reprobed with anti-Akt/PkBα or anti-GSK3α/ß antibody to determine the total Akt and GSK3α/ß levels. The immunoreactive proteins were visualized using SuperSignal West Pico Chemiluminescent substrate Protein bands were scanned and the band densities were quantified by using ImageJ (NIH, 1.48v) software.

Metabolic labeling to detect SERT phosphorylation

Phosphorylated [^{32}P]SERT was immunoisolated and quantified as described previously [29, 44]. Briefly, HEK 293 cells expressing hSERT were metabolically labeled with [^{32}P]orthophosphate in phosphate-free DMEM for 1 hour and incubated with Akt X (20 μM) for 15 min at 37°C. The cells were washed and solubilized with RIPA buffer containing protease and phosphatase Inhibitors (composition given above). The SERT proteins were immunoprecipitated using SERT specific antibody SR-12. The immunoprecipitated proteins were isolated by the addition of protein A-Sepharose beads, washed three times with RIPA buffer and the proteins were eluted in 45 μl of Laemmli sample buffer for 30 min at 22°C. The eluted proteins were separated by SDS-PAGE (10%). Gels were dried and exposed to Kodak BioMax Ms-1 films and ^{32}P-radiolabeled SERT was visualized by autoradiography. The SERT bands were quantified by using ImageJ (NIH, 1.48v) software as described previously by this laboratory [29, 44].

Immunostaining

Transiently transfected HEK 293 cells were pretreated with 20 μM Akt X in KRH as described for the uptake assay. Subsequently, the cells were washed in PBS and fixed with 4% paraformaldehyde for 15 min at room temperature. The samples were washed in PBS before blocking with 1% bovine serum albumin (BSA) in PBS, and permeabilized using 0.2% saponin. The sample was stained for hSERT using goat-anti SERT (1:100), lysosome using rabbit anti-Lamp1 (1:800), Golgi using rabbit anti-giantin (1:800), and ER-Golgi intermediate compartment using rabbit anti-ERGIC53 (1:500) as well as donkey anti-rabbit-Alexa488 and donkey anti-goat-Alexa568. The samples were then mounted in *ProLong Gold Antifade* reagent (Molecular Probes, Invitrogen).

Confocal microscopy

Confocal microscopy was performed with an inverted Zeiss LSM 510 laser-scanning unit (Carl Zeiss, Oberkochen, Germany) through an oil immersion 63× 1.4 numerical aperture objective (Carl Zeiss). AlexaFluor 488 and EGFP were excited using a 488 nm argon-krypton laser and the emitted light was filtered through a 505-530 nm band-pass filter. The AlexaFluor 568 was excited using a 543 nm helium-neon laser and the emitted light was filtered using a 560 nm long-pass filter. For co-localizations studies, images were acquired using line shift, and an averaging of 8. Images were collected in 1024x1024 pixels and pinholes were set to achieve optical sections of 1 μm.

Quantitative co-localization microscopy

The amount of internalization was calculated using ImageJ software. A mask was created to remove background using permanent settings for each image. The remaining intracellular fluorescence was normalized to the total remaining

fluorescence. In each individual experiment, the average intracellular fraction of vehicle treated cells was normalized to 1. Statistical significance was determined by a two-sample t-test with a Welch correction. Data are mean ± standard error of the mean (S.E.M.). Data are from 52-69 cells from three independent experiments. Co-localization was studied utilizing Van Steensel's cross-correlation fraction with the JACoP plug-in [45]. The red and green image was split into the two channels, and a mask was generated for each color to remove background light before measuring the cross-correlation. Van Steensel's cross correlation function was determined by calculating the Pearson's coefficient (PC) in a given overlay of the two images, and then shifting one of the colors 20 pixels in each x direction compared to the other, plotting PC as a function of the pixel shift (Δx). Complete overlay gives a cross-correlation function of 1 at Δx = 0. Co-localization was determined based on 18 cells from three independent experiments. Data are mean ± standard error of the mean (S.E.M.).

Statistical analyses

Values are expressed as mean ± SEM. As noted in the figure legends, one-way or two-way analysis of variance was used followed by *post hoc* testing (Bonferroni) for multiple comparisons. Student's *t* test was performed for comparison between two groups. Prism 6 (GraphPad, San Diego, CA) was used for data analysis. A value of $P < 0.05$ was considered statistically significant.

RESULTS

Akt inhibition reduces SERT activity

Using Akt X, which inhibits Akt activity [46] we asked whether protein kinase B/Akt regulates SERT function. Akt X treatment of the HEK 293 cells, transiently expressing hSERT, reduced 5-HT uptake in a dose and time dependent manner (Fig 1A & B). When varying concentrations of Akt X (1, 2.5, 5, 10 and 20 μM) were tested for 30 min, a dose dependent decrease in 5-HT uptake is evident ($F_{(5,42)} = 12.95$; $p < 0.0001$) (Fig. 1A). A Bonferroni's post hoc analysis revealed that 5, 10 and 20 μM Akt X produced significant decrease in 5-HT uptake ($p \leq 0.01$) compared to vehicle treated cells. Preincubation of cells with 2.5, 5, 10 and 20 μM of Akt X for 30 min produced 16%, 27%, 32% and 55% inhibition of 5-HT uptake respectively (Fig 1A). When cells were treated with 10 μM of Akt X for 5, 15, 30 and 60 min at 37°C prior to [^{3}H] 5HT uptake assay, a time dependent decrease in 5-HT uptake was observed ($F_{(4,44)} = 9.04$; $p < 0.0001$) (Fig. 1B). A Bonferroni's post hoc analysis revealed that a significant decrease in 5-HT uptake is evident at 5 min pretreatment of Akt X (20%; $p \leq 0.05$) and reached maximum inhibition at 30 min pretreatment (38%; $p \leq 0.0001$). To verify that Akt X inhibits Akt activity that is correlated with SERT activity inhibition, we examined the phosphorylation status of Akt (Ser-473). As shown in Fig. 1C, immunoblotting of cell lysates showed significantly reduced levels of phospho-Akt ($p \leq 0.02$; N=3) in cells treated with Akt X (20 μM, 30 min) with no significant change in the total Akt protein. These results indicate that acute inhibition of Akt activity leads to decreased SERT activity.

Specific Knock-down of Akt by siRNA reduces SERT activity

To further support our findings that Akt regulates SERT activity, we used short interfering RNA targeting Akt and determined the effect of loss of function of Akt on 5-HT uptake. Forty hours after transfection of siRNAs, total Akt ($t=3.72$, $df=11$, $p<0.003$) as well as phospho-Akt (Ser-473) ($t=3.66$, $df=7$, $p<0.008$) were significantly reduced in cells transfected with Akt-siRNA/hSERT compared to cells transfected with nonspecific scrambled siRNA/hSERT (Fig. 2A, B). Akt-siRNA and/or scrambled siRNA transfection did not affect the total expression of calnexin (Fig. 2A) ruling out any non-specific effects. In parallel experiments, a significant reduction in 5-HT uptake was observed in cells transfected with Akt-siRNA/hSERT compared to that observed in cells transfected with nonspecific scrambled siRNA/hSERT ($t=4.86$, $df=16$, $p<0.0002$) (Fig. 2C). Consistent with Akt X results (Fig. 1), the results from the specific genetic knockdown of Akt (Fig. 2) strongly support the idea that endogenous Akt plays a crucial role in the regulation of SERT activity.

Akt inhibition reduces SERT mediated 5-HT uptake capacity

The kinetic parameters (Michaelis-Menten constant, K_m and V_{max}) of SERT were determined using vehicle and Akt X (20 μM, 30 min) treated HEK 293 cells expressing hSERT (Fig. 3). Akt X treatment produced a significant reduction (~26%) in the maximal velocity (V_{max}) compared to vehicle treated cells ($t=2.6$, $df=6$, $p<0.04$). The V_{max} in vehicle treated cells is 3263 ± 249 fmol/10^6cells/min and in Akt X treated cells is 2408 ± 215 fmol/10^6cells/min. Interestingly, Akt X exposure did not change SERT affinity for its substrate 5-HT ($p<0.99$). K_m values obtained were 180 ± 52.67 and 180.8 ± 38.87 nM for vehicle treated and Akt X treated cells respectively (Fig 3).

Akt inhibition reduces cell surface density of SERT

Next we sought to determine whether Akt X mediated down regulation of SERT activity is attributed to reduced surface SERT levels, using membrane impermeable protein biotinylating agents. Surface SERT levels were determined using HEK 293 cells expressing hSERT following treatment with vehicle or Akt X. Figure 4 shows that the Akt X treatment (20 μM, 45 min) decreased cell surface expression of SERT. Quantification of surface SERT immunoreactive band densities revealed a significant decrease (~38%, $t=3.51$, $df=8$, $p<0.008$) in the amount of surface SERT (Fig. 4). Total SERT level did not change following Akt X exposure. Calnexin protein expression was not affected by Akt X treatment or not present in biotinylated fractions (not shown). Thus the reduction in surface SERT protein correlated with the reduction in the transport capacity V_{max} as measured by 5-HT uptake (Fig. 3).

Akt inhibition reduces SERT plasma membrane delivery without affecting the internalization

Akt X-induced decrease in SERT cell surface expression could arise from reduced plasma membrane insertion, or enhanced endocytosis of SERT or a combination of both. Therefore, we investigated the effect of Akt X on SERT plasma membrane insertion (exocytosis) and SERT internalization using biotinylation strategy as described previously by us [40]. Figure 5A shows the results of biotinylation experiments in which newly inserted SERT levels to the plasma membrane following Akt X or vehicle treatment. To evaluate the delivery of SERT to the cell surface, first pre-existing surface SERTs were blocked from biotinylation by treating cells with sulfo-NHS acetate. Sulfo-NHS acetate treatment at 4°C blocks all the free amino groups on the proteins that will be biotinylated otherwise [42, 43]. No biotinylated

SERT was present at the zero time point in sulfo-NHS acetate treated cells suggesting that all pre-existing surface SERTs are blocked (from modification by biotinylation). Therefore, any biotinylated SERT observed at subsequent time points after warming the cells to 37ºC represents newly delivered SERT only. In vehicle treated cells there was a gradual, time-dependent increase in SERT plasma membrane insertion which plateaued at the 30 min time point ($F_{(3,25)} = 4.36$; $p < 0.02$). This increase represents constitutive transporter delivery to the plasma membrane. Akt X treatment significantly decreased constitutive plasma membrane recycling of SERT ($F_{(7,39)} = 5.05$; $p < 0.0004$). While a Bonferroni's post hoc analysis revealed a significant decrease in SERT delivery was apparent at 15 and 30 min following Akt X treatment ($p < 0.03$, 0.04 respectively), a trend in non-significant decrease in SERT delivery was evident at 2.5 and 5 min following Akt X treatment (Fig. 5A). These results indicate that Akt activity regulates SERT plasma membrane delivery.

We next examined the internalization of SERT under basal/constitutive conditions, and following treatment with Akt X using the reversible biotinylation strategy and by quantifying the fraction of surface biotinylated-SERT that moves in a time-dependent manner to an intracellular compartment. Biotin from remaining biotinylated proteins on the surface at the end of a particular treatment protocol was removed by treatment with MesNa, a non-permeant reducing agent that reduces disulfide bonds and liberates biotin from biotinylated proteins at the cell surface. Thus the amount of biotinylated proteins inaccessible to MesNa action is defined as "the amount of protein endocytosed or internalized". The amount of SERT biotinylated in the absence of MesNa represents total biotinylated transporter. MesNa treatment immediately after biotinylation showed less than 2-3% of total biotinylated SERT indicating very little internalization at 4°C (Fig 5B, lane 1 vs 2 from left). Following vehicle treatment, a gradual, time-dependent increase in biotinylated SERT was observed in vehicle treated cells (Fig. 5B). This increase in internalized SERT represents basal or constitutive SERT endocytosis. However, Akt X did not significantly affect SERT endocytosis when compared to vehicle treatment (Fig. 5B). The results from exocytosis and endocytosis assay collectively demonstrate that inhibition of Akt decreases cell surface SERT and that reduced SERT plasma membrane insertion contributes to reduced SERT mediated 5-HT uptake.

Intracellularly accumulated hSERT co-localizes with markers of lysosomal degradation

In order to investigate the intracellular accumulation of hSERT in Akt X treated cells, we performed immunocytochemistry on hSERT in transiently transfected HEK 293 cells. The cells were treated with 20 μM Akt X for 45 min at 37°C or vehicle prior to immunocytochemistry. Confocal imaging of the cells showed that hSERT primarily localized to the plasma membrane of the HEK 293 cells with only low levels of intracellular transporter (Fig. 6A, left). In agreement with the biochemical data, we also observed that treatment with Akt X led to the appearance of multiple hSERT positive vesicular structures in the cytoplasm of the transfected cells (Fig. 6A, right, yellow arrowheads). Notably, quantification of this intracellular accumulation suggested a significant 6-fold increase ($p<0.0001$; 52-69 cells from three independent experiments) in intracellular hSERT accumulation in the Akt X treated cells compared to vehicle treated cells (Fig. 6B).

To investigate the nature of the intracellular compartment to which hSERT co-localized upon AKT X treatment, we first performed co-staining with antibodies targeting the endoplasmic reticulum-Golgi intermediate compartment (ERGIC53), the Golgi apparatus (giantin), and lysosomes (Lamp1). Our imaging suggested no accumulation of hSERT positive vesicles in neither ERGIC nor Golgi (Fig. 7A, white arrows). However, a marked number of hSERT positive vesicles were positive also for Lamp1, indicating partial accumulation of hSERT in the lysosomal pathway upon treatment with AKT X (Fig. 7A, yellow arrows). For quantification of the imaging, we used Van Steensel's cross correlation function, which calculates the Pearson coefficient as it shifts the two color images across each other and plots the cross-correlation. No peak was observed for ERGIC and Golgi in agreement with no co-localization. In contrast, there was for Lamp1 a sharp peak at $\Delta x = 0$ (cross-correlation value 0.15), suggesting partial, but specific, overlap between hSERT and Lamp1 (Fig. 7B). One way ANOVA with a Bonferroni's post hoc multiple comparisons established significant difference between Lamp1 and ERGIC as well as Giantin ($p<0.0001$)

Next, we performed co-transfections with small Rab GTPases (Rab)s tagged with enhanced green fluorescent protein (EGFP). The EGFP-Rab constructs can be used as markers of distinct endocytic compartments. Rab4 mediates fast recycling from the early endosome to the plasma membrane and has therefore been utilized as marker for the early endosome and the 'short recycling loop'. Rab5 is involved in fusion with the early endosome and is thus also used as a marker for the early endosome. Because Rab7 is enriched in compartments of the late endosome and mediates the maturation of the late endosome as well as the fusion with the lysosome it is used as a marker of the late endosome/lysosome and lysosomal degradation. Finally, Rab11 marks the 'long recycling loop' through the recycling endosomes (reviewed in [47]). The confocal imaging showed some overlay of the hSERT immunosignal with the markers of the early endosome (Rab4 and Rab5a) and the short recycling loop (Rab4) (Fig. 8A, yellow arrowheads). However, the co-localization of hSERT with EGFP-Rab7, and thus late endosomes, appeared more prominent whereas the co-localization of the hSERT signal and EGFP-Rab11 was very limited (Fig. 8A, yellow arrowheads). One way ANOVA with a Bonferroni's post hoc multiple comparisons revealed a significant difference between Rab7 and Rab11 ($p<0.01$). This pattern was supported by the cross-correlation analysis supporting the strongest specific co-localization of hSERT with EGFP-Rab7 (cross-correlation value ~0.17) followed by EGFP-Rab5 (cross-correlation value ~0.125) and EGFP-Rab4 (cross-correlation value ~0.10). For EGFP-Rab11, the cross-correlation value was only 0.05 (Fig. 8B). Taken together, the data suggest that hSERT accumulates upon AKT X treatment in intracellular endocytic compartments with the most prominent localization to late endosomes and lysosomes.

Akt2/PKBß inhibition reduces SERT activity

Three mammalian isoforms of Akt have been identified (reviewed in [48]). We took a pharmacological approach to identify the involvement of Akt1 and Akt2 by treating hSERT expressing HEK 293 cells with different concentrations of Akt1 inhibitor A-674563 and Akt2 inhibitor CCT128930 for 45 min at 37°C [49, 50]. SERT activity measured from Akt1 and Akt2 inhibitor treated cells showed a dose dependent decrease in 5-HT uptake at varying degrees (Fig. 9). The decrease in SERT activity was influenced by dose and its interaction with Akt1 or Akt2 inhibitor (two-way

analysis of variance; interaction: ($F_{(5,64)}$ =5.94; $p < 0.0001$); dose: ($F_{(1,64)}$ =45.11; $p < 0.0001$) and drug (Akt1, Akt2 inhibitors) ($F_{(5,64)}$ =30.56; $p < 0.0001$)). Subsequent Bonferroni's post hoc multiple analysis revealed that while 1 μM Akt2 inhibitor CCT128930 caused significant inhibitory effect on SERT activity (~31%; $p \leq 0.01$), Akt1 inhibitor A-674563 produced equivalent inhibitory effect (~36%, $p \leq 0.01$) only at higher (5 μM) concentrations. In addition, the results revealed that Akt2 inhibitor CCT128930 was more potent than Akt1 inhibitor A-674563 in inhibiting SERT activity (Fig. 9).

Glycogen synthase kinase-3α/ß inhibition stimulates SERT activity

Because activated Akt phosphorylates and inactivates glycogen synthase kinase-3α/ß (GSK3α/ß) [33, 51], we therefore examined whether Akt regulates SERT function through modulating GSK3α/ß. We assessed the effect of three known inhibitors specific to GSK3α/β (TDZD-8, CHIR-99021 and BIO [52-54]) on SERT-mediated 5-HT uptake in HEK 293 cells expressing hSERT. Figure 10A showed that treatment of various concentrations of GSK3α/β inhibitors for 45 min resulted in significantly higher SERT activity (Bonferroni's post hoc multiple analysis: $F_{(9,55)}$ =7.10; $p < 0.0001$). In parallel, we tested the efficacy of CHIR-99021 on phospho-GSK3α/β levels. It has been reported that GSK3 inhibitors cause an increase in the phosphorylation of GSK3α/β (Ser-21 and Ser-9 respectively) to inhibit GSK3α/ß activity [55]. Consistent with published reports, our representative Western blot (Fig. 10B) show that treatment of CHIR-99021 increased phospho-levels of GSK3α/β suggesting decreased GSK3α/β activities. These results demonstrated that inhibition of GSK3α/β activity enhances SERT activity.

Akt inhibition reduces SERT basal phosphorylation

Since SERT regulation is linked to transporter phosphorylation [10, 15, 16, 19, 29, 44], we hypothesized that phosphorylation of SERT may contribute to Akt X-induced downregulation of SERT function and surface expression. To test this, phosphorylation of SERT was examined following treatment with Akt X or vehicle in HEK 293 cells expressing hSERT. Consistent with our previous reports [44], using SERT specific antibody and SDS-PAGE/autoradiography of immunoprecipitates from [^{32}P]-metabolically labeled cells expressing hSERT revealed ^{32}P-labeled SERT (~96 kDa) in vehicle treated cells (Fig. 11). This represents basal SERT phosphorylation. Interestingly, treatment with Akt X (20 μM, 30 min) significantly reduced the level of SERT basal phosphorylation (by 58.7%; $t=4.71$, $df=8$; $p<0.0015$) suggesting the role of Akt in regulating SERT basal phosphorylation.

DISCUSSION

Depression has been associated with serotoninergic dysfunction in the central nervous system [9] and the major determinant of 5-HT signaling is the SERT. Altered expression and function of SERT is known in many disease states such as anxiety, depression, OCD, autism, irritable bowel syndrome and hypertension [6-9]. Thus, understanding the signaling molecules and pathways involved in the regulation of SERT is of importance. Altered Akt activity and Akt substrate glycogen synthase kinase-3ß (GSK-3ß) have been implicated in depressed suicide victims [31, 32]. It is possible that Akt may regulate SERT function to maintain normal synaptic 5-HT.

However, whether Akt activity regulates SERT function has yet to be investigated. Because of the implication of Akt and SERT in mood disorders, it became important to investigate whether Akt mediated SERT function played any role in 5-HT uptake. Current study, for the first time identifies the involvement of Akt in SERT regulation. Pharmacological reduction in the activity of Akt with Akt inhibitor Akt X inhibited SERT activity. Akt X is an N^{10}-substituted phenoxanzine, which inhibits Akt activity by blocking Akt phosphorylation [46]. Additionally, genetic knockdown of Akt significantly reduces SERT function. Moreover, Akt X- and siRNA- mediated inhibition of Akt phosphorylation correlated with the inhibition of SERT activity. The combined pharmacological and genetic data indicate that Akt plays a role in the regulation of SERT function.

Accumulating evidence indicates that modulating SERT internalization and membrane insertion are attributable to altered surface level of SERT expression. In current report, we found that Akt inhibition is associated with a significant reduction in SERT V_{max} without affecting substrate affinity. This suggested the possibility of altered surface abundance of SERT protein. Supporting this, we observed that a loss of surface SERT protein after Akt X treatment. Confocal microscopy approach revealed a significant 6-fold increase in intracellular SERT accumulation in Akt X treated cells supporting further that Akt inhibition decreases 5-HT uptake through decreasing functional SERT protein on the plasma membrane. Greater intracellular SERT is observed in confocal imaging than decreased surface SERT from surface biotinylation/immunoblot. This may be due to the differences associated with different assays employed or sampling bias inherent in the single-cell imaging relative to the population determination of biotinylated surface SERT by immunoblot. Akt X treatment did not change the total expression of SERT protein suggesting that SERT redistribution rather than loss of total SERT protein via degradation or reduced SERT synthesis. We previously demonstrated that activation of PKC or inhibition of p38 MAPK decreased surface abundance of SERT [12, 15, 16]. On the other hand Src-mediated tyrosine phosphorylation of SERT regulates SERT stability and 5-HT transport [17, 21]. Perhaps, the most compelling cellular events in kinase mediated amine transporter regulation involve changes in transporter protein internalization and membrane insertion resulting in the change in surface transporter density. We previously showed that while PKC activation triggers SERT internalization, p38 MAPK inhibition impede the membrane insertion of SERT suggesting distinct trafficking mechanisms involved in PKC and p38 MAPK mediated SERT surface regulation [16]. It is noteworthy that p38 MAPK may also participate in catalytic activation of SERT through an unknown mechanism [18]. Adapting cell surface biotin labeling of newly delivered SERT to plasma membrane and reversible biotinylation strategy to follow internalized biotin tagged-SERT, we gathered evidence that Akt inhibition decreases SERT plasma membrane delivery with no significant effect on SERT internalization. Additionally, imaging of co-localization of SERT with intracellular organelle revealed that Akt X treatment increased SERT co-immunosignal with the markers for the lysosome (Lamp1), early endosome (Rab4 and Rab5a), short recycling loop (Rab4) and the late endosomes (Rab7), but not with the Golgi (Giantin) or endoplasmic reticulum (ERGIC) markers. Notably, SERT co-localization with Lamp1 and Rab7 were more predominant than others. These data suggest that activity of Akt regulates SERT trafficking pathways at the level of intracellular organelle such as late endosomes and lysosomes and possibly others and thereby regulating SERT delivery to plasma membrane and subsequent 5-HT

transport. Of interest, recent data have suggested that hSERT upon constitutive internalization is sorted primarily to late endosomes/ lysosomes [56] and thus it is possible that the Akt associated SERT subcellular distribution occurs through the same pathway. Pharmacological inhibition of Akt1 and Akt2 indicates that SERT is more sensitive to Akt2 inhibitor than Akt1 and thus both isoforms are likely to be involved in the regulation of SERT. However the involvement of Akt3 isoform cannot be ruled out. Clearly, further studies are needed to firmly confirm the Akt isoforms that involved in SERT regulation. Akt inactivates its downstream kinase GSK3α/β [33, 51]. Therefore, it is possible that Akt may regulate SERT through inhibiting GSK3α/β activity. Since Akt inhibition inhibits SERT, Akt activation and subsequent inhibition of GSK3α/β should stimulate SERT. Consistent with this notion, all three GSK3α/β inhibitors tested elevated SERT activity suggesting that involvement of Akt-modulated GSK3α/β in SERT regulation. Since several signaling pathways converge to regulate GSK3α/β (reviewed in [33, 57-59]), alternative possible mechanism is that Akt and GSK3α/β may regulate SERT independently through distinct mechanisms or in conjunction with other signaling pathways. Further detailed studies are needed to establish these possibilities.

SERT is a phospho-protein and several kinases including PKC, PKA, PKG, CaMK, p38 MAPK and Src regulate the phosphorylation of SERT [10, 15, 16, 19, 29, 44, 60]. We have shown that phosphorylation of Thr-276 residue in SERT by activated PKG upregulates SERT function [19]. Both Akt and GSK3α/β are serine-threonine kinases, and it is possible that Akt and GSK3α/β regulate SERT intracellular trafficking via SERT phosphorylation. The current finding that inhibition of Akt decreases SERT basal phosphorylation suggests a role for Akt in the regulation of SERT phosphorylation. Further studies are warranted to determine whether Akt-GSK3α/β phosphorylates SERT directly and to determine the motifs involved and the role of Akt-mediated SERT phosphorylation in SERT trafficking and function.

Autoreceptors (5-HT_{1A} and 5-HT_{1B}) and heteroreceptor (TrkB) exist on serotonergic neurons to activate Akt [61-64]. It is well known that activation of 5-HT_{1A} and 5-HT_{1B} influences 5-HT release and firing rates (reviewed [65] reference therein). Furthermore, BDNF-TrkB signaling is critical for synaptic plasticity [66, 67]. While signaling pathways were not described, it has been reported that activation of 5-HT_{1B} or TrkB receptors increases 5-HT clearance [25, 26, 68]. The observations and findings from the current study suggest that receptors on serotonergic neurons may influence SERT redistribution through Akt-GSK3α/β pathways in order to maintain normal 5-HT neurotransmission. Therefore, it is tempting to speculate that Akt-GSK3α/β mediated SERT regulation may serve as one of the mechanisms for functional plasticity at serotonergic terminals. Further studies are needed (i) to identify signaling pathways upstream and downstream of Akt and GSK3α/β, (ii) to delineate how post-translational modifications of SERT are affected by Akt and GSK3α/β signaling, and (iii) to define the role of Akt and GSK3α/β-dependent SERT modifications in SERT trafficking and function.

Abnormal regulations of SERT, 5-HT signaling and BDNF-TrkB signaling have been implicated in the pathophysiology of mood disorders [6-9, 65, 69-75]. Of interest is that genetic variants of Akt and Akt1-binding protein (AKTIP) are

associated with suicidal behavior and depression [30-32]. Notably, altered GSK3ß phosphorylation [76] and polymorphism in the GSK3ß promoter [77] has been implicated in depression/suicide and mood disorders. In this regard, the current study identifies the involvement of Akt and GSK3α/β signaling pathway in SERT regulation and underscores the biological importance because any perturbation in the normal regulation of SERT might have functional consequences on 5-HT-linked signaling and behavior.

AUTHOR CONTRIBUTION

Jeyaganesh Rajamanickam, Balasubramaniam Annamalai, Troels Rahbek-Clemmensen and Santhanalakshmi Sundaramurthy conducted experiments, acquired data and performed data analysis. Jeyaganesh Rajamanickam and Troels Rahbek-Clemmensen drafted the manuscript. Lankupalle Jayanthi, Ulrik Gether and Sammanda Ramamoorthy critically revised the manuscript prior to submission.

FUNDING

This work was supported by the National Institute of Health grants MH062612, MH083928, MH091633 and start up fund from Virginia Commonwealth University (S.R.).

REFERENCES

1 O'Reilly, C. A. and Reith, M. E. (1988) Uptake of [3H]serotonin into plasma membrane vesicles from mouse cerebral cortex. J. Biol. Chem. **263**, 6115-6121
2 Povlock, S. L. and Amara, S. G. (1997) The structure and function of norepinephrine, dopamine, and serotonin transporters. In Neurotransmitter Transporters: Structure, Function, and Regulation (Reith, M. E. A., ed.). pp. 1-28, Humana Press, Totowa, NJ
3 Barker, E. L. and Blakely, R. D. (1995) Norepinephrine and serotonin transporters: Molecular targets of antidepressant drugs. Psychopharmacology: The Fourth Generation of Progress, 321-333
4 Ramamoorthy, S., Bauman, A. L., Moore, K. R., Han, H., Yang-Feng, T., Chang, A. S., Ganapathy, V. and Blakely, R. D. (1993) Antidepressant- and cocaine-sensitive human serotonin transporter: molecular cloning, expression, and chromosomal localization. Proc. Natl. Acad. Sci. U. S. A. **90**, 2542-2546
5 Rudnick, G. and Wall, S. C. (1992) The molecular mechanism of "ecstasy" [3,4-methylenedioxy-methamphetamine (MDMA)]: serotonin transporters are targets for MDMA-induced serotonin release. Proc. Natl. Acad. Sci. U. S. A. **89**, 1817-1821
6 Insel, T. R., Zohar, J., Benkelfat, C. and Murphy, D. L. (1990) Serotonin in obsessions, compulsions, and the control of aggressive impulses. Ann. N. Y. Acad. Sci. **600**, 574-585; discussion 585-576
7 Meltzer, H. Y. (1990) Role of serotonin in depression. Ann. N. Y. Acad. Sci. **600**, 486-499; discussion 499-500
8 Cook, E. H., Jr. and Leventhal, B. L. (1996) The serotonin system in autism. Curr. Opin. Pediatr. **8**, 348-354
9 Murphy, D. L., Lerner, A., Rudnick, G. and Lesch, K. P. (2004) Serotonin transporter: gene, genetic disorders, and pharmacogenetics. Mol Interv. **4**, 109-123

10 Ramamoorthy, S., Shippenberg, T. S. and Jayanthi, L. D. (2011) Regulation of monoamine transporters: Role of transporter phosphorylation. Pharmacol. Ther. **129**, 220-238
11 Jayanthi, L. D., Ramamoorthy, S., Mahesh, V. B., Leibach, F. H. and Ganapathy, V. (1994) Calmodulin-dependent regulation of the catalytic function of the human serotonin transporter in placental choriocarcinoma cells. J. Biol. Chem. **269**, 14424-14429
12 Qian, Y., Galli, A., Ramamoorthy, S., Risso, S., DeFelice, L. J. and Blakely, R. D. (1997) Protein kinase C activation regulates human serotonin transporters in HEK-293 cells via altered cell surface expression. J. Neurosci. **17**, 45-57
13 Bauman, A. L., Apparsundaram, S., Ramamoorthy, S., Wadzinski, B. E., Vaughan, R. A. and Blakely, R. D. (2000) Cocaine and antidepressant-sensitive biogenic amine transporters exist in regulated complexes with protein phosphatase 2A. J. Neurosci. **20**, 7571-7578
14 Ramamoorthy, S. (2002) Regulation of monoamine transporters: Regulated phosphorylation, dephosphorylation and Trafficking. In Neurotransmitter transporter: Structure, function and regulation (Reith, M. E. A., ed.). pp. 1-23, Humana
15 Jayanthi, L. D., Samuvel, D. J., Blakely, R. D. and Ramamoorthy, S. (2005) Evidence for biphasic effects of protein kinase C on serotonin transporter function, endocytosis, and phosphorylation. Mol. Pharmacol. **67**, 2077-2087
16 Samuvel, D. J., Jayanthi, L. D., Bhat, N. R. and Ramamoorthy, S. (2005) A role for p38 mitogen-activated protein kinase in the regulation of the serotonin transporter: evidence for distinct cellular mechanisms involved in transporter surface expression. J. Neurosci. **25**, 29-41
17 Zarpellon, A., Donella-Deana, A., Folda, A., Turetta, L., Pavanetto, M. and Deana, R. (2008) Serotonin (5-HT) transport in human platelets is modulated by Src-catalysed Tyr-phosphorylation of the plasma membrane transporter SERT. Cell. Physiol. Biochem. **21**, 87-94
18 Zhu, C. B., Carneiro, A. M., Dostmann, W. R., Hewlett, W. A. and Blakely, R. D. (2005) p38 MAPK activation elevates serotonin transport activity via a trafficking-independent, protein phosphatase 2A-dependent process. J. Biol. Chem. **280**, 15649-15658
19 Ramamoorthy, S., Samuvel, D. J., Buck, E. R., Rudnick, G. and Jayanthi, L. D. (2007) Phosphorylation of threonine residue 276 is required for acute regulation of serotonin transporter by cyclic GMP. J. Biol. Chem. **282**, 11639-11647
20 Chanrion, B., Mannoury la Cour, C., Bertaso, F., Lerner-Natoli, M., Freissmuth, M., Millan, M. J., Bockaert, J. and Marin, P. (2007) Physical interaction between the serotonin transporter and neuronal nitric oxide synthase underlies reciprocal modulation of their activity. Proc. Natl. Acad. Sci. U. S. A. **104**, 8119-8124
21 Annamalai, B., Mannangatti, P., Arapulisamy, O., Shippenberg, T. S., Jayanthi, L. D. and Ramamoorthy, S. (2012) Tyrosine phosphorylation of the human serotonin transporter: a role in the transporter stability and function. Mol. Pharmacol. **81**, 73-85
22 Miller, K. J. and Hoffman, B. J. (1994) Adenosine A3 receptors regulate serotonin transport via nitric oxide and cGMP. J. Biol. Chem. **269**, 27351-27356
23 Zhu, C. B., Hewlett, W. A., Feoktistov, I., Biaggioni, I. and Blakely, R. D. (2004) Adenosine receptor, protein kinase G, and p38 mitogen-activated protein kinase-dependent up-regulation of serotonin transporters involves both transporter trafficking and activation. Mol. Pharmacol. **65**, 1462-1474

24 Matheus, N., Mendoza, C., Iceta, R., Mesonero, J. E. and Alcalde, A. I. (2009) Regulation of serotonin transporter activity by adenosine in intestinal epithelial cells. Biochem. Pharmacol. **78**, 1198-1204
25 Daws, L. C., Gould, G. G., Teicher, S. D., Gerhardt, G. A. and Frazer, A. (2000) 5-HT(1B) receptor-mediated regulation of serotonin clearance in rat hippocampus in vivo. J. Neurochem. **75**, 2113-2122.
26 Benmansour, S., Deltheil, T., Piotrowski, J., Nicolas, L., Reperant, C., Gardier, A. M., Frazer, A. and David, D. J. (2008) Influence of brain-derived neurotrophic factor (BDNF) on serotonin neurotransmission in the hippocampus of adult rodents. Eur. J. Pharmacol. **587**, 90-98
27 Launay, J. M., Bondoux, D., Oset-Gasque, M. J., Emami, S., Mutel, V., Haimart, M. and Gespach, C. (1994) Increase of human platelet serotonin uptake by atypical histamine receptors. Am. J. Physiol. **266**, R526-536
28 Ansah, T. A., Ramamoorthy, S., Montanez, S., Daws, L. C. and Blakely, R. D. (2003) Calcium-dependent inhibition of synaptosomal serotonin transport by the alpha 2-adrenoceptor agonist 5-bromo-N-[4,5-dihydro-1H-imidazol-2-yl]-6-quinoxalinamine (UK14304). J. Pharmacol. Exp. Ther. **305**, 956-965
29 Ramamoorthy, S. and Blakely, R. D. (1999) Phosphorylation and sequestration of serotonin transporters differentially modulated by psychostimulants. Science. **285**, 763-766
30 Magno, L. A., Miranda, D. M., Neves, F. S., Pimenta, G. J., Mello, M. P., De Marco, L. A., Correa, H. and Romano-Silva, M. A. (2010) Association between AKT1 but not AKTIP genetic variants and increased risk for suicidal behavior in bipolar patients. Genes Brain Behav. **9**, 411-418
31 Hsiung, S. C., Adlersberg, M., Arango, V., Mann, J. J., Tamir, H. and Liu, K. P. (2003) Attenuated 5-HT1A receptor signaling in brains of suicide victims: involvement of adenylyl cyclase, phosphatidylinositol 3-kinase, Akt and mitogen-activated protein kinase. J. Neurochem. **87**, 182-194
32 Karege, F., Perroud, N., Burkhardt, S., Schwald, M., Ballmann, E., La Harpe, R. and Malafosse, A. (2007) Alteration in kinase activity but not in protein levels of protein kinase B and glycogen synthase kinase-3beta in ventral prefrontal cortex of depressed suicide victims. Biol. Psychiatry. **61**, 240-245
33 Beaulieu, J. M., Gainetdinov, R. R. and Caron, M. G. (2009) Akt/GSK3 signaling in the action of psychotropic drugs. Annu. Rev. Pharmacol. Toxicol. **49**, 327-347
34 Li, X., Rosborough, K. M., Friedman, A. B., Zhu, W. and Roth, K. A. (2007) Regulation of mouse brain glycogen synthase kinase-3 by atypical antipsychotics. Int. J. Neuropsychopharmacol. **10**, 7-19
35 Li, X., Zhu, W., Roh, M. S., Friedman, A. B., Rosborough, K. and Jope, R. S. (2004) In vivo regulation of glycogen synthase kinase-3beta (GSK3beta) by serotonergic activity in mouse brain. Neuropsychopharmacology. **29**, 1426-1431
36 Barreto, R. A., Walker, F. R., Dunkley, P. R., Day, T. A. and Smith, D. W. (2012) Fluoxetine prevents development of an early stress-related molecular signature in the rat infralimbic medial prefrontal cortex. Implications for depression? BMC Neurosci. **13**, 125
37 Beaulieu, J. M., Zhang, X., Rodriguiz, R. M., Sotnikova, T. D., Cools, M. J., Wetsel, W. C., Gainetdinov, R. R. and Caron, M. G. (2008) Role of GSK3 beta in behavioral abnormalities induced by serotonin deficiency. Proc. Natl. Acad. Sci. U. S. A. **105**, 1333-1338

38 Lavezzari, G., McCallum, J., Dewey, C. M. and Roche, K. W. (2004) Subunit-specific regulation of NMDA receptor endocytosis. J. Neurosci. **24**, 6383-6391
39 Brown, T. C., Correia, S. S., Petrok, C. N. and Esteban, J. A. (2007) Functional compartmentalization of endosomal trafficking for the synaptic delivery of AMPA receptors during long-term potentiation. J. Neurosci. **27**, 13311-13315
40 Jayanthi, L. D., Annamalai, B., Samuvel, D. J., Gether, U. and Ramamoorthy, S. (2006) Phosphorylation of the norepinephrine transporter at threonine 258 and serine 259 is linked to protein kinase C-mediated transporter internalization. J. Biol. Chem. **281**, 23326-23340
41 Zapata, A., Kivell, B., Han, Y., Javitch, J. A., Bolan, E. A., Kuraguntla, D., Jaligam, V., Oz, M., Jayanthi, L. D., Samuvel, D. J., Ramamoorthy, S. and Shippenberg, T. S. (2007) Regulation of dopamine transporter function and cell surface expression by D3 dopamine receptors. J. Biol. Chem. **282**, 35842-35854
42 Lee-Kwon, W., Kawano, K., Choi, J. W., Kim, J. H. and Donowitz, M. (2003) Lysophosphatidic acid stimulates brush border Na+/H+ exchanger 3 (NHE3) activity by increasing its exocytosis by an NHE3 kinase A regulatory protein-dependent mechanism. J. Biol. Chem. **278**, 16494-16501
43 Peng, Y., Amemiya, M., Yang, X., Fan, L., Moe, O. W., Yin, H., Preisig, P. A., Yanagisawa, M. and Alpern, R. J. (2001) ET(B) receptor activation causes exocytic insertion of NHE3 in OKP cells. Am. J. Physiol. Renal Physiol. **280**, F34-42
44 Ramamoorthy, S., Giovanetti, E., Qian, Y. and Blakely, R. D. (1998) Phosphorylation and regulation of antidepressant-sensitive serotonin transporters. J. Biol. Chem. **273**, 2458-2466
45 Bolte, S. and Cordelieres, F. P. (2006) A guided tour into subcellular colocalization analysis in light microscopy. J. Microsc. **224**, 213-232
46 Thimmaiah, K. N., Easton, J. B., Germain, G. S., Morton, C. L., Kamath, S., Buolamwini, J. K. and Houghton, P. J. (2005) Identification of N10-substituted phenoxazines as potent and specific inhibitors of Akt signaling. J. Biol. Chem. **280**, 31924-31935
47 Stenmark, H. (2009) Rab GTPases as coordinators of vesicle traffic. Nat. Rev. Mol. Cell Biol. **10**, 513-525
48 Brazil, D. P. and Hemmings, B. A. (2001) Ten years of protein kinase B signalling: a hard Akt to follow. Trends Biochem. Sci. **26**, 657-664
49 Bottermann, K., Reinartz, M., Barsoum, M., Kotter, S. and Godecke, A. (2013) Systematic Analysis Reveals Elongation Factor 2 and alpha-Enolase as Novel Interaction Partners of AKT2. PLoS One. **8**, e66045
50 Luo, Y., Shoemaker, A. R., Liu, X., Woods, K. W., Thomas, S. A., de Jong, R., Han, E. K., Li, T., Stoll, V. S., Powlas, J. A., Oleksijew, A., Mitten, M. J., Shi, Y., Guan, R., McGonigal, T. P., Klinghofer, V., Johnson, E. F., Leverson, J. D., Bouska, J. J., Mamo, M., Smith, R. A., Gramling-Evans, E. E., Zinker, B. A., Mika, A. K., Nguyen, P. T., Oltersdorf, T., Rosenberg, S. H., Li, Q. and Giranda, V. L. (2005) Potent and selective inhibitors of Akt kinases slow the progress of tumors in vivo. Mol. Cancer Ther. **4**, 977-986
51 Cross, D. A., Alessi, D. R., Cohen, P., Andjelkovich, M. and Hemmings, B. A. (1995) Inhibition of glycogen synthase kinase-3 by insulin mediated by protein kinase B. Nature. **378**, 785-789
52 Martinez, A., Alonso, M., Castro, A., Perez, C. and Moreno, F. J. (2002) First non-ATP competitive glycogen synthase kinase 3 beta (GSK-3beta) inhibitors: thiadiazolidinones (TDZD) as potential drugs for the treatment of Alzheimer's disease. J. Med. Chem. **45**, 1292-1299

53 Bennett, C. N., Ross, S. E., Longo, K. A., Bajnok, L., Hemati, N., Johnson, K. W., Harrison, S. D. and MacDougald, O. A. (2002) Regulation of Wnt signaling during adipogenesis. J. Biol. Chem. **277**, 30998-31004
54 Polychronopoulos, P., Magiatis, P., Skaltsounis, A. L., Myrianthopoulos, V., Mikros, E., Tarricone, A., Musacchio, A., Roe, S. M., Pearl, L., Leost, M., Greengard, P. and Meijer, L. (2004) Structural basis for the synthesis of indirubins as potent and selective inhibitors of glycogen synthase kinase-3 and cyclin-dependent kinases. J. Med. Chem. **47**, 935-946
55 Liang, M. H. and Chuang, D. M. (2007) Regulation and function of glycogen synthase kinase-3 isoforms in neuronal survival. J. Biol. Chem. **282**, 3904-3917
56 Rahbek-Clemmensen, T., Bay, T., Eriksen, J., Gether, U. and Jorgensen, T. N. (2014) The serotonin transporter undergoes constitutive internalization and is primarily sorted to late endosomes and lysosomal degradation. J. Biol. Chem. **289**, 23004-23019
57 Doble, B. W. and Woodgett, J. R. (2003) GSK-3: tricks of the trade for a multi-tasking kinase. J. Cell Sci. **116**, 1175-1186
58 Grimes, C. A. and Jope, R. S. (2001) The multifaceted roles of glycogen synthase kinase 3beta in cellular signaling. Prog. Neurobiol. **65**, 391-426
59 Frame, S. and Cohen, P. (2001) GSK3 takes centre stage more than 20 years after its discovery. Biochem. J. **359**, 1-16
60 Seimandi, M., Seyer, P., Park, C. S., Vandermoere, F., Chanrion, B., Bockaert, J., Mansuy, I. M. and Marin, P. (2013) Calcineurin interacts with the serotonin transporter C-terminus to modulate its plasma membrane expression and serotonin uptake. J. Neurosci. **33**, 16189-16199
61 Leone, A. M., Errico, M., Lin, S. L. and Cowen, D. S. (2000) Activation of extracellular signal-regulated kinase (ERK) and Akt by human serotonin 5-HT(1B) receptors in transfected BE(2)-C neuroblastoma cells is inhibited by RGS4. J. Neurochem. **75**, 934-938
62 Cowen, D. S., Johnson-Farley, N. N. and Travkina, T. (2005) 5-HT receptors couple to activation of Akt, but not extracellular-regulated kinase (ERK), in cultured hippocampal neurons. J. Neurochem. **93**, 910-917
63 Madhav, T. R., Pei, Q. and Zetterstrom, T. S. (2001) Serotonergic cells of the rat raphe nuclei express mRNA of tyrosine kinase B (trkB), the high-affinity receptor for brain derived neurotrophic factor (BDNF). Brain Res. Mol. Brain Res. **93**, 56-63
64 Chao, M. V., Rajagopal, R. and Lee, F. S. (2006) Neurotrophin signalling in health and disease. Clin. Sci. (Lond.). **110**, 167-173
65 Pineyro, G. and Blier, P. (1999) Autoregulation of serotonin neurons: role in antidepressant drug action. Pharmacol. Rev. **51**, 533-591.
66 Mamounas, L. A., Altar, C. A., Blue, M. E., Kaplan, D. R., Tessarollo, L. and Lyons, W. E. (2000) BDNF promotes the regenerative sprouting, but not survival, of injured serotonergic axons in the adult rat brain. J. Neurosci. **20**, 771-782
67 Pittenger, C. and Duman, R. S. (2008) Stress, depression, and neuroplasticity: a convergence of mechanisms. Neuropsychopharmacology. **33**, 88-109
68 Mossner, R., Daniel, S., Albert, D., Heils, A., Okladnova, O., Schmitt, A. and Lesch, K. P. (2000) Serotonin transporter function is modulated by brain-derived neurotrophic factor (BDNF) but not nerve growth factor (NGF). Neurochem. Int. **36**, 197-202
69 Stockmeier, C. A., Shapiro, L. A., Dilley, G. E., Kolli, T. N., Friedman, L. and Rajkowska, G. (1998) Increase in serotonin-1A autoreceptors in the midbrain of

suicide victims with major depression-postmortem evidence for decreased serotonin activity. J. Neurosci. **18**, 7394-7401
70 Kernie, S. G. and Parada, L. F. (2000) The molecular basis for understanding neurotrophins and their relevance to neurologic disease. Arch. Neurol. **57**, 654-657
71 Schmidt, H. D., Banasr, M. and Duman, R. S. (2008) Future Antidepressant Targets: Neurotrophic Factors and Related Signaling Cascades. Drug Discov. Today Ther. Strateg. **5**, 151-156
72 Duman, R. S. and Monteggia, L. M. (2006) A neurotrophic model for stress-related mood disorders. Biol. Psychiatry. **59**, 1116-1127
73 Castren, E., Voikar, V. and Rantamaki, T. (2007) Role of neurotrophic factors in depression. Curr. Opin. Pharmacol. **7**, 18-21
74 Naughton, M., Mulrooney, J. B. and Leonard, B. E. (2000) A review of the role of serotonin receptors in psychiatric disorders. Hum Psychopharmacol. **15**, 397-415
75 Cryan, J. F. and Leonard, B. E. (2000) 5-HT1A and beyond: the role of serotonin and its receptors in depression and the antidepressant response. Hum Psychopharmacol. **15**, 113-135
76 Karege, F., Perroud, N., Burkhardt, S., Fernandez, R., Ballmann, E., La Harpe, R. and Malafosse, A. (2012) Protein levels of beta-catenin and activation state of glycogen synthase kinase-3beta in major depression. A study with postmortem prefrontal cortex. J. Affect. Disord. **136**, 185-188
77 Serretti, A., Benedetti, F., Mandelli, L., Calati, R., Caneva, B., Lorenzi, C., Fontana, V., Colombo, C. and Smeraldi, E. (2008) Association between GSK-3beta -50T/C polymorphism and personality and psychotic symptoms in mood disorders. Psychiatry Res. **158**, 132-140

FIGURE LEGENDS

Figure 1 Regulation of 5-HT uptake by Akt X

(A) Dose dependence. Transiently transfected HEK 293 cells with hSERT were pretreated with assay buffer alone (vehicle) and different concentration of Akt X for 30 min at 37°C followed by 5 min [^{3}H]5-HT (50 nM) uptake. Values are expressed as mean ± S.E.M. *p< 0.05, **p< 0.01, ***p< 0.0001 compared with vehicle (One-Way ANOVA with Bonferroni multiple comparison test). (**B)** Time course. Transiently transfected HEK 293 cells were pretreated with 20 µM Akt X for the times indicated and assayed for [^{3}H]5-HT (50 nM) uptake for 5 min at 37°C. Values are expressed as mean ± S.E.M. *p< 0.05, **p< 0.01, ***p< 0.0001 compared with vehicle (One-Way ANOVA with Bonferroni multiple comparison test). The results are shown as percentage of specific SERT mediated uptake values relative to the uptake observed in vehicle control as described under "*Methods*" section. **(C)** Representative immunoblot (top panel) showing phospho-Akt, total Akt in vehicle and Akt X (20 µM, 30 min) treated cells. The data shown in bottom panel are statistical analysis of normalized (phopho-Akt/total Akt) band densities from three separate experiments. *P< 0.0 compared with vehicle (Student's *t* test). Veh, vehicle.

Figure 2 Effect of siRNA knock-down of Akt expression on 5-HT transport

HEK 293 cells were transfected with 30 nM siRNAs targeted to Akt or control scrambled siRNAs before the transfection of hSERT as described under "*Methods*"

section. Transfected cells were used for 5-HT transport, total Akt and phospho-Akt expression. **(A)** Representative Western blot from separate experiments shows the expression levels of total Akt (N=6) and phospho-Akt (N=5) and calnexin. **(B)** Average band densities of total and phospho-Akt and data represent mean ± S.E.M. **p< 0.01 compared with scrambled siRNAs plus hSERT transfected cells (Student's *t* test). **(C)** SERT specific 5-HT uptake values, and data represent mean ± S.E.M. SERT specific 5-HT uptake was performed as described in "*Methods*" and in the legend to Fig.1). ***p< 0.0002, (N=9) significantly different scrambled siRNAs plus hSERT transfected cells (Student's *t* test).

Figure 3 Effect of Akt X on SERT mediated 5-HT uptake kinetics

HEK 293 cells transiently transfected with hSERT were pretreated with vehicle or Akt X (20 μM, 30 min). After the treatment, uptake of 5-HT was quantified over a concentration range of 25 nM to 2500 nM using a 5 min uptake period. Nonspecific uptake at each concentration of 5-HT used (in the presence of 0.01 μM fluoxetine) was subtracted from total uptake (measured in the absence of fluoxetine) to calculate SERT mediated 5-HT uptake. Values are the averages from three different experiments and the mean values ± S.E.M. are given. Nonlinear curve fits of data for uptake used the generalized Michaelies-Menten equation (Prism GraphPad).

Figure 4 Cell surface SERT density

HEK 293 cells transiently transfected with hSERT were pretreated with vehicle or Akt X (20 μM, 45 min). After the treatment, biotinylation with EZ-link sulfo-NHS-SS-biotin was performed. Biotinylated fractions, and total fractions were subjected to SDS-PAGE followed by immunoblotting with SERT specific SR-12 antibody as described under "*Methods*" section. A representative SERT immunoblot of four different experiments is shown (top panel). Bar graph shows quantified SERT band densities (bottom panel). Values are expressed as mean ± S.E.M. **p<0.008 versus vehicle control (Student's *t* test).

Figure 5 Effect of Akt X on SERT exocytosis and endocytosis

(A) SERT exocytosis/plasma membrane insertion. HEK 293 cells expressing hSERT were treated with sulfo-NHS-acetate to block all free amino groups prior to biotinylation with sulfo-NHS-SS-biotin in the presence of vehicle or Akt X (20 μM, 45 min) for the indicated time periods. Isolation of biotinylated and nonbiotinylated proteins and immunoblotting of SERT were performed as described under *"Methods"* section. A representative blot (top panel) shows changes in biotinylated SERT following Akt X and vehicle treatments. Biotinylated SERT bands were quantified using NIH ImageJ, and mean (± S.E.M) band densities are shown in the lower panel (Bar graphs). ∗ p< 0.05 indicates significant changes in the SERT exocytosis following Akt X treatment compared to corresponding vehicle treatment at each time point (One-Way ANOVA with Bonferroni multiple comparison test). **(B)** SERT endocytosis/internalization. Cells were biotinylated with sulfo-NHS-SS-biotin and incubated with vehicle or 20 μM Akt X for the times indicated. Following MesNa treatment, biotinylated (internalized) SERTs were isolated and analyzed as described under *"Methods"* section. Representative immunoblots from three separate experiments are given in upper panels. The bar graphs show biotinylated SERT levels. The densities of SERT bands from three separate experiments are given as mean ± S.E.M. p=0.39, no significant effect on SERT internalization

following Akt X treatment (One-Way ANOVA with Bonferroni multiple comparison test).

Figure 6. Effect of Akt X on hSERT cellular distribution

HEK 293 cells transiently transfected with hSERT were serum starved for 2 hours and treated with vehicle or Akt X (20 μM, 45 min at 37°C) before fixation. The samples were visualized by antibody labeling targeting the C-terminal tail of SERT using confocal microscopy. **(A)** Images of hSERT in vehicle or Akt X treated HEK 293 cells. Images are representative of three independent experiments. Yellow arrowheads mark intracellular accumulation. **(B)** Quantification of the intracellular levels of hSERT. A mask was generated for each cell based on a fixed intensity, in order to remove background fluorescence. A ROI was generated measuring the intracellular levels as a ratio of the total fluorescence from each cell. In each individual experiment was the average intracellular level of vehicle treated cells normalized to 1. Significance was determined by a two-sample t-test with a Welch correction ($p<0.0001$). Data are means of 52-69 cells from three independent experiments.

Figure 7. Co-localization of intracellular hSERT with ERGIC, Golgi, and Lysosome

HEK 293 cells transiently expressing hSERT were serum starved and treated with Akt X (20 μM, 45 min at 37°C) before fixation. **(A)** The cells were stained with antibodies targeting hSERT using Alexa568-labelled secondary antibody and ERGIC (ERGIC53), Golgi (Giantin), and lysosome (Lamp1) using Alexa488-labelled antibody. Images are representative of three independent experiments. White arrows mark hSERT positive compartments that do not co-localize, and yellow arrowheads mark co-localization between hSERT and Lamp1. **(B)** Quantification of the hSERT co-localization with ERGIC, Golgi, and lysosome using Van Steensel's cross-correlation function. This approach determines the cross-correlation for the movement of two images relative to each other. A sharp peak at $\Delta x = 0$ represents co-localization. Values less than 1 show partial co-localization. Data represents 18 cells for each cellular marker from three independent experiments.

Figure 8. Co-localization of intracellular hSERT with EGFP-labelled markers of endocytic compartments.

HEK 293 cells transiently expressing hSERT and EGFP-labelled Rab4, Rab5a, Rab7, or Rab11 were serum starved and treated with Akt X (20 μM, 45 min at 37°C) before fixation. **(A)** The cells were stained with antibodies targeting hSERT using Alexa568-labelled secondary antibody. Images are representative of three independent experiments. Yellow arrowheads mark co-localization between hSERT and endocytic markers **(B)** Quantification of the hSERT co-localization with EGFP-Rab4, -Rab5a, -Rab7, or -Rab11 using Van Steensel's cross-correlation function. This approach determines the cross-correlation for the movement of two images relative to each other. A sharp peak at $\Delta x = 0$ represents co-localization. Values less than 1 show partial co-localization. The peak gets taller as the amount of co-localization increases. Data represents 18 cells for each cellular marker from three independent experiments

Figure 9. Effect of Akt1 and Akt2 inhibitors on SERT activity.

Transiently transfected HEK 293 cells with hSERT were pretreated with vehicle (DMSO) or different concentrations of Akt1 inhibitor A-674563 or Akt2 inhibitor CCT128930 for 40 min at 37°C followed by 5 min [^{3}H]5-HT (50 nM) uptake. Values are expressed as mean ± S.E.M. *p< 0.05, **p< 0.01, ***p< 0.0001 compared with corresponding vehicle, ^p< 0.05, ^^p< 0.01, ^^^p< 0.0001 values significantly different from equivalent Akt1 inhibitor A-674563 concentration (Two-Way ANOVA with Bonferroni multiple comparison test).

Figure 10. Effect of GSK3α/ß inhibitors on SERT activity.

(A) Transiently transfected HEK 293 cells with hSERT were pretreated with vehicle or different concentration of GSK3α/ß inhibitors, BIO, CHIR-99021 and TDZD-8 for 40 min at 37°C followed by 5 min [^{3}H]5-HT (50 nM) uptake (A). Values are expressed as mean ± S.E.M. *p< 0.05, **p< 0.01 compared with the respective vehicle control (One-Way ANOVA with Bonferroni multiple comparison test). (B) Representative Western blots from three separate experiments show the levels of total and phospho GSK3α/ß using specific antibodies.

Figure 11. Effect of Akt X on SERT phosphorylation.

HEK 293 cells were transiently transfected with hSERT cDNA. After 24 hours post transfection, cells were metabolically labeled with [^{32}]orthophosphate in phosphate-free DMEM for 1 hour and incubated with 20 μM Akt X for 15 min. RIPA extraction, immunoprecipitation, SDS-PAGE and autoradiography were performed as described under "*Methods*" section. An autoradiogram of ^{32}P-labeled hSERT (~96 kDa), representative of five experiments, is shown (top panel). Quantification of ^{32}P-labeled SERT bands as arbitrary units were given in bar graph (bottom panel). $^{**}p$ <0.001 (N=5) compared with vehicle (Student's *t* test).

Biochemical Journal Immediate Publication. Published on 11 Mar 2015 as manuscript BJ20140826

Figure 1

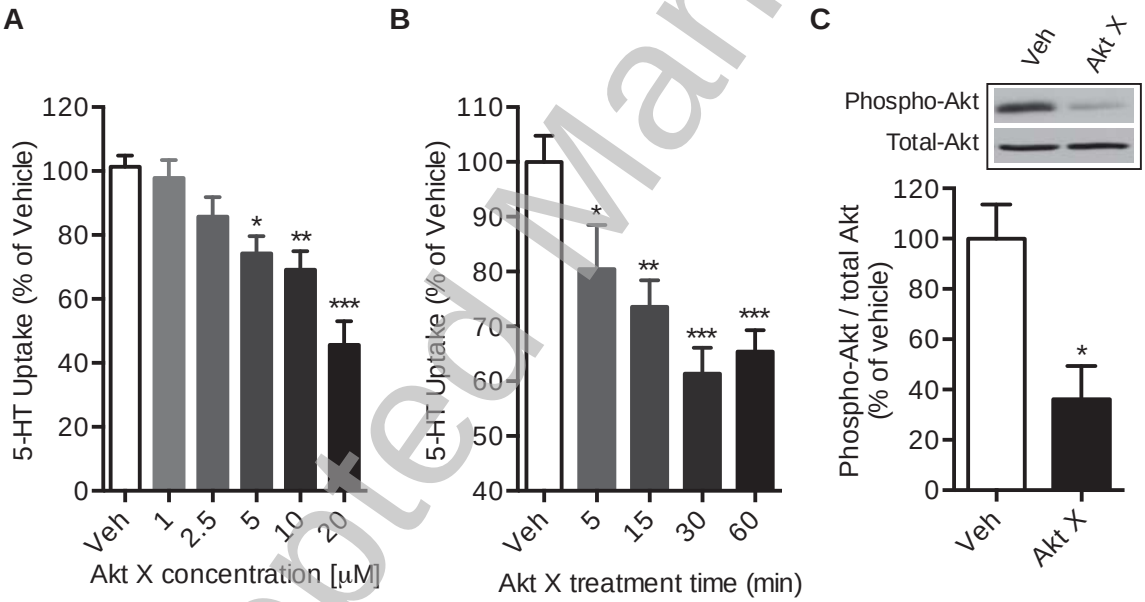

Biochemical Journal Immediate Publication. Published on 11 Mar 2015 as manuscript BJ20140826

Figure 2

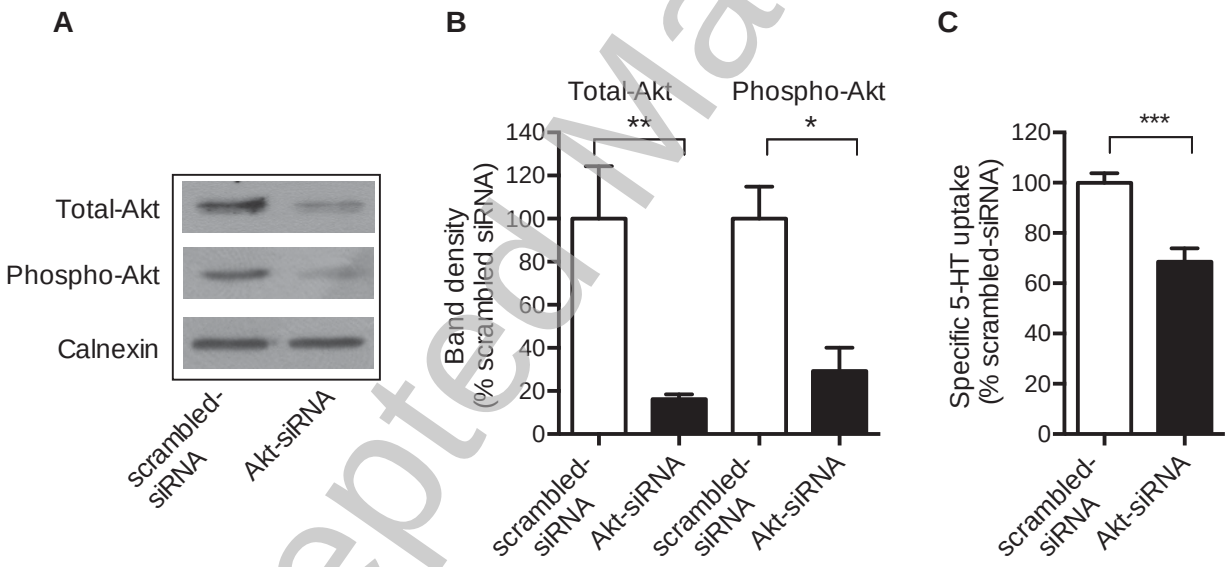

Figure 3

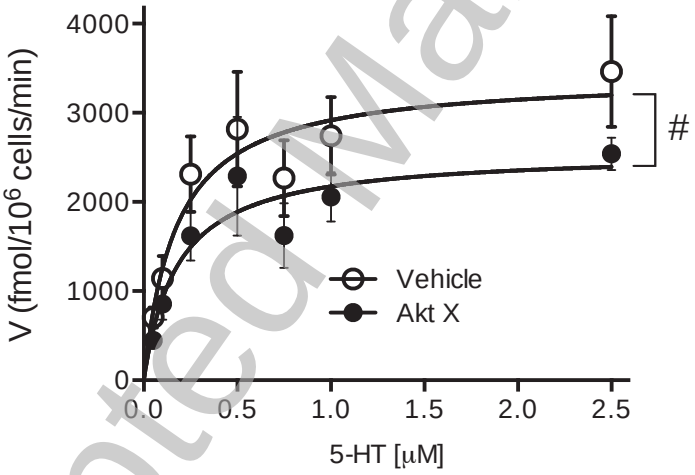

Biochemical Journal Immediate Publication. Published on 11 Mar 2015 as manuscript BJ20140826

Figure 4

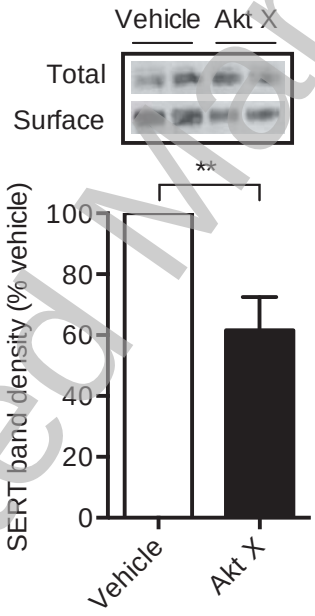

Figure 5

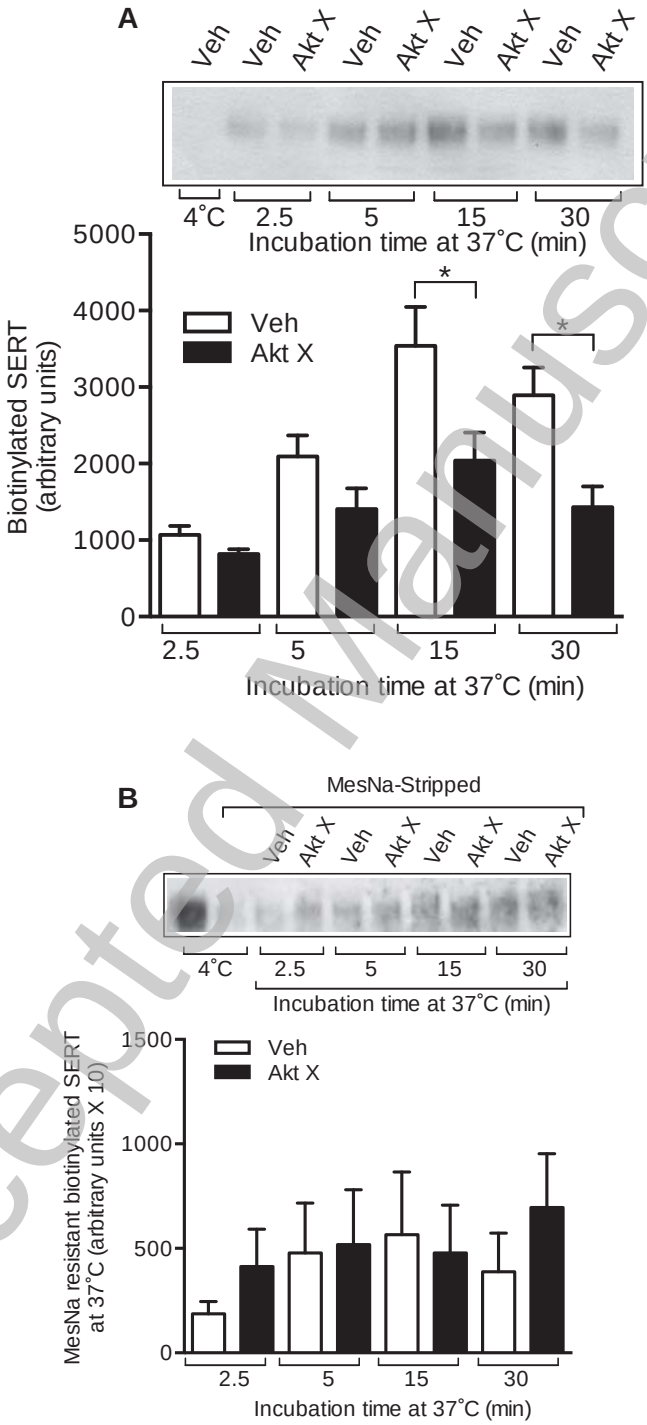

Biochemical Journal Immediate Publication. Published on 11 Mar 2015 as manuscript BJ20140826

Figure 6

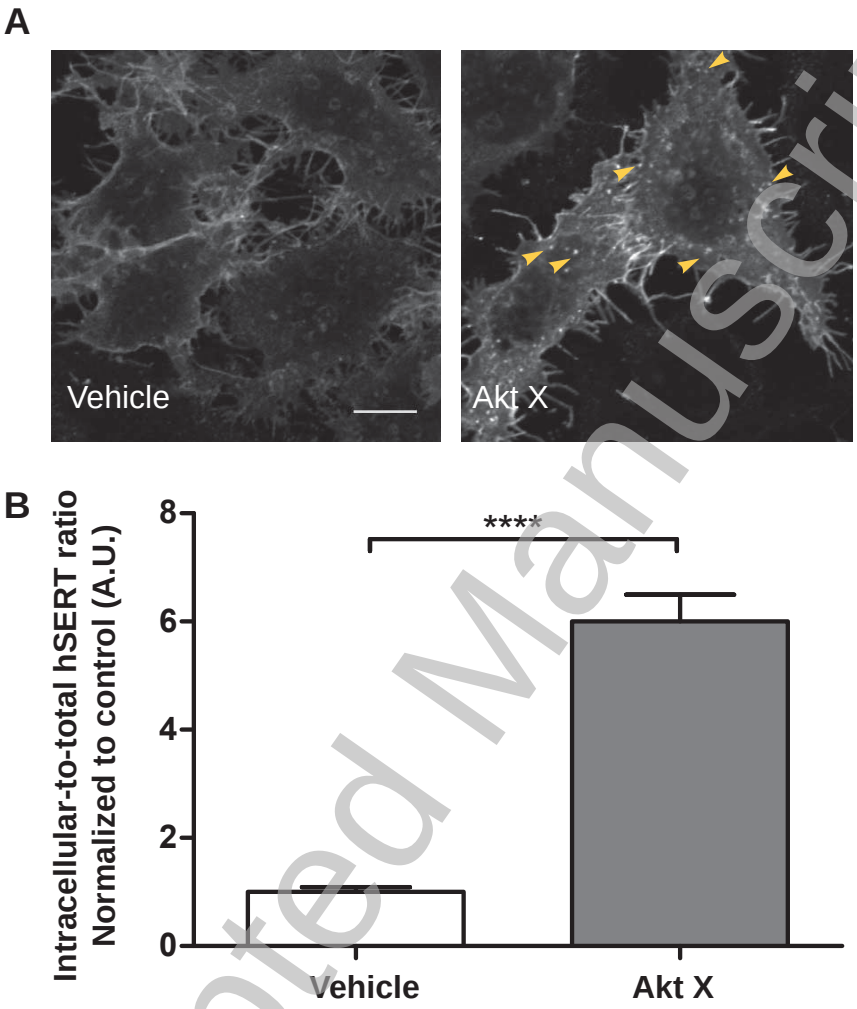

Biochemical Journal Immediate Publication. Published on 11 Mar 2015 as manuscript BJ20140826

Figure 7

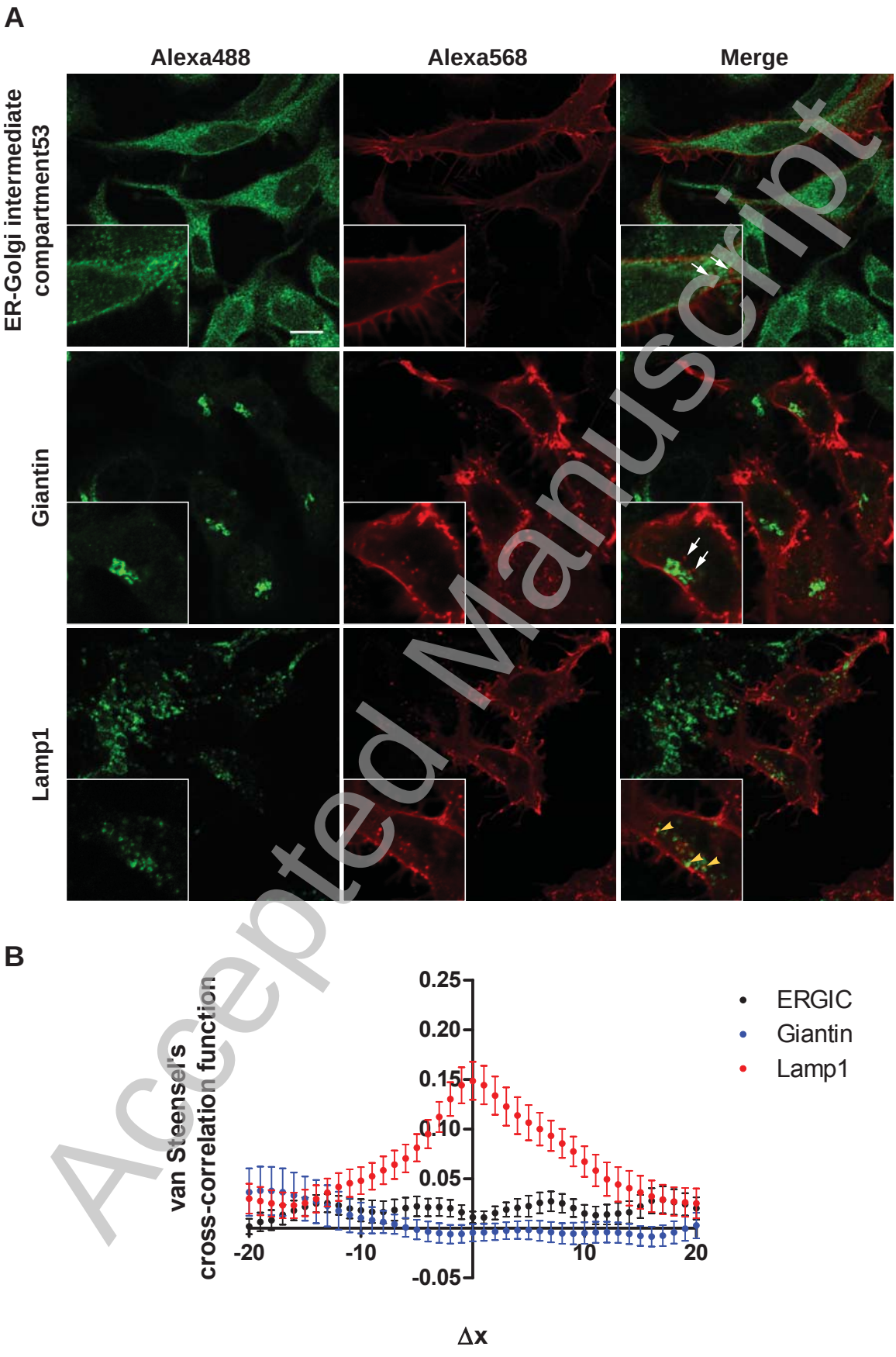

Biochemical Journal Immediate Publication. Published on 11 Mar 2015 as manuscript BJ20140826

Figure 8

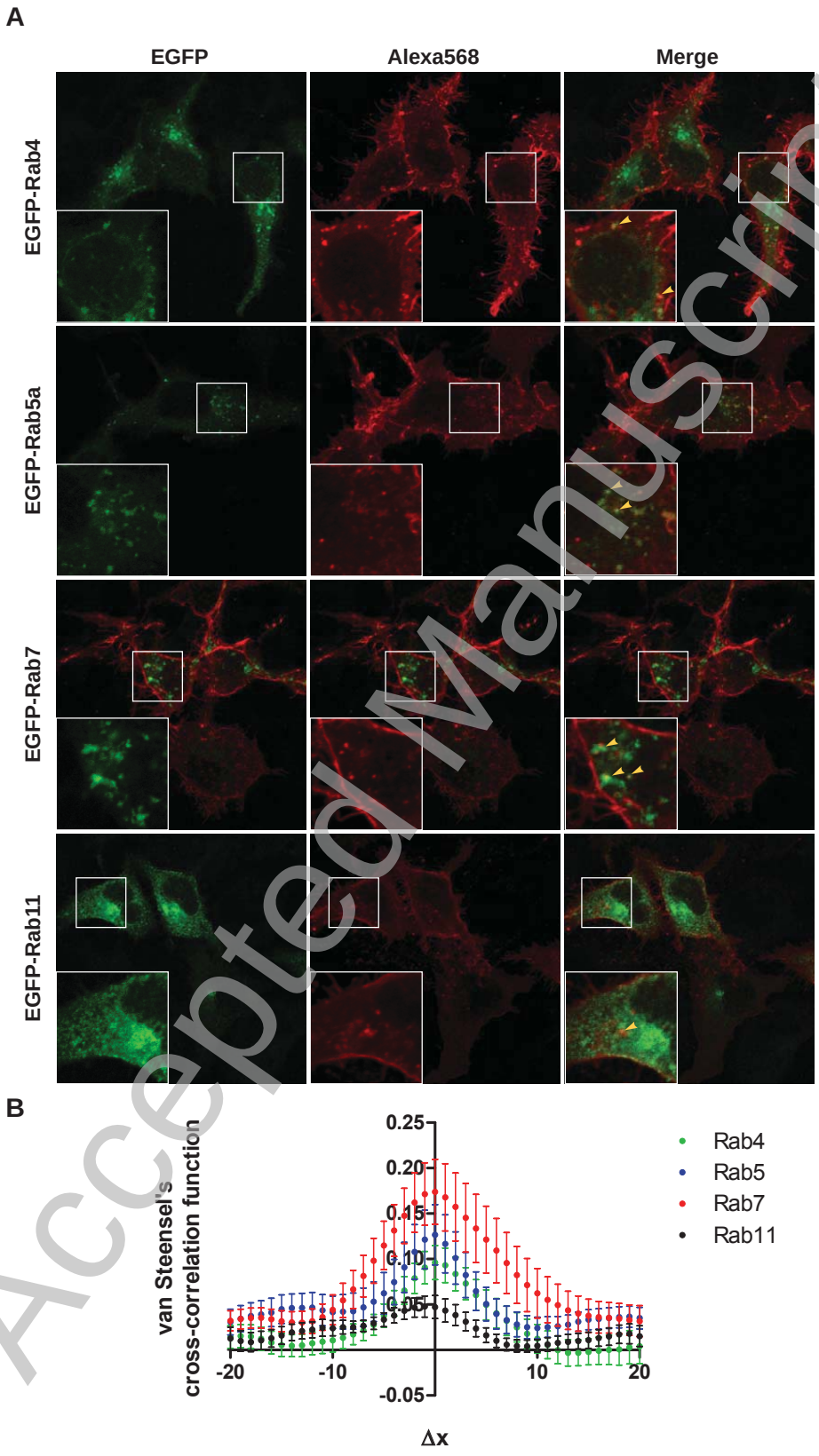

Biochemical Journal Immediate Publication. Published on 11 Mar 2015 as manuscript BJ20140826

Figure 9

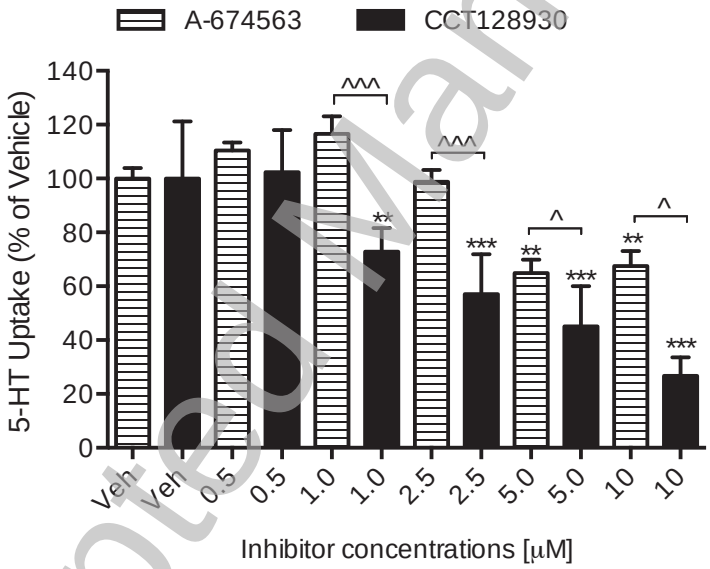

Biochemical Journal Immediate Publication. Published on 11 Mar 2015 as manuscript BJ20140826

Figure 10

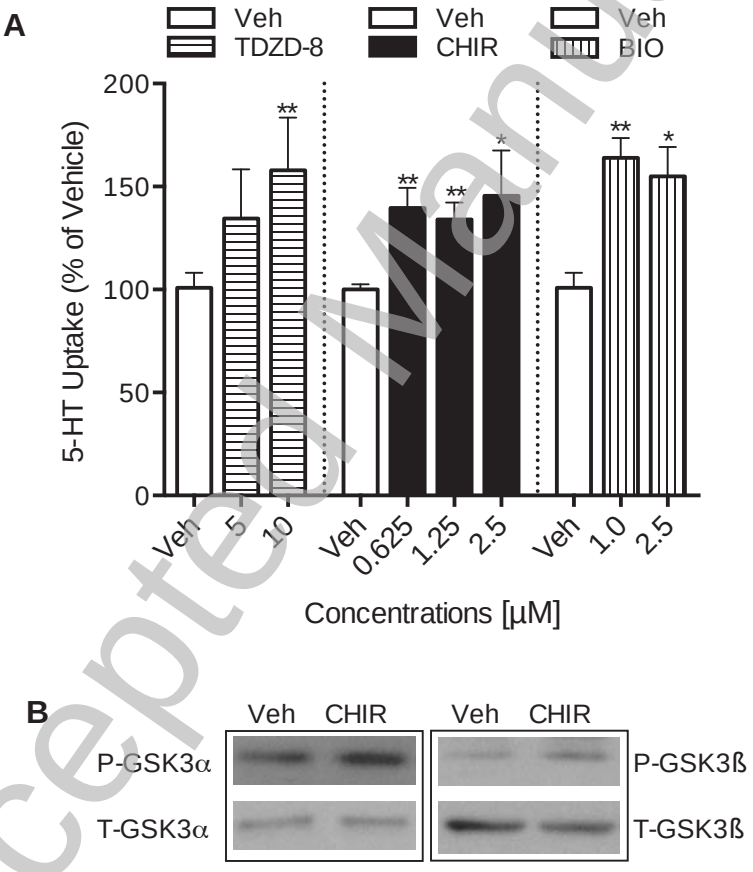

Biochemical Journal Immediate Publication. Published on 11 Mar 2015 as manuscript BJ20140826

Figure 11